UNIVERSITAT ROVIRA I VIRGILI
DESIGN, FABRICATION AND CHARACTERIZATION OF POROUS SILICON MULTILAYER OPTICAL DEVICES
Elisabet Xifré Pérez
ISBN: 978-84-691-0362-3/DL: T.2181-2007

Chapter 4

Analysis and design of optical devices based on porous silicon multilayers

In this chapter, the study and design of multilayer optical devices are presented. These optical devices are omnidirectional mirrors and waveguides. For the case of omnidirectional mirrors, in addition to the known periodic multilayer structure, three different new multilayer structures are proposed for the widening of the omnidirectional bandgap. For the case of waveguides, the modal study of porous silicon waveguides based on total internal reflection is developed. Waveguides based on the properties of photonic crystals are also widely studied, proposing the use of omnidirectional mirrors and DBR for their cladding. All these multilayer optical devices have been designed for 1.55 μm applications and the use of porous silicon for their fabrication is discussed. For this study, the simulation programs explained in the previous chapter have been used.

UNIVERSITAT ROVIRA I VIRGILI
DESIGN, FABRICATION AND CHARACTERIZATION OF POROUS SILICON MULTILAYER OPTICAL DEVICES
Elisabet Xifré Pérez
ISBN: 978-84-691-0362-3/DL: T.2181-2007

4.1. Omnidirectional mirrors (OM)

Omnidirectional mirrors are characterized by their omnidirectional bandgap, that is the wavelength range where the reflectivity is the unity for any incidence angle and any polarization. The width of the omnidirectional bandgap depends on the structure of the mirror.

In the next sections, multilayer omnidirectional mirrors with different structures based on porous silicon are studied for 1.55 μm applications. They are explained and mathematically analyzed using the transfer matrix method [151]. The aim of this study is the design of a porous silicon mirror with an enlarged omnidirectional bandgap. Firstly, the widely used periodic mirror is presented and studied. Next, the fairly used chirped structure is described and its advantages are evaluated. Finally, the analysis and study of the random structure lead us to two new OM structures with an enlarged omnidirectional bandgap: the balanced and the unbalanced mirrors.

4.1.1. Periodic OM

The multilayer structure most commonly used for the formation of omnidirectional mirrors is the periodic structure [110-112,116]. Ideally, it is an infinitely extended multilayer consisting of the periodic repetition of two different refractive index layers n_H and n_L and thicknesses h_H and h_L, respectively. The period thickness or bilayer thickness of the structure is $\Lambda=h_H+h_L$, and the refractive index profile is given by $n(x)=n(x+\Lambda)$.

Porous silicon periodic OMs have been simulated and analyzed. From the study of these structures, the presence and width of the omnidirectional bandgap has been observed to depend mainly on three different factors.

4.1.1.1. Refractive indices n_H and n_L

The existence of one or more omnidirectional bandgaps depends on the refractive indices n_H and n_L of the mirror [161]. This dependence can be observed in the examples presented in Fig. 4.1. This figure shows the projected

UNIVERSITAT ROVIRA I VIRGILI
DESIGN, FABRICATION AND CHARACTERIZATION OF POROUS SILICON MULTILAYER OPTICAL DEVICES
Elisabet Xifré Pérez
ISBN: 978-84-691-0362-3/DL: T.2181-2007

band structure (PBS) of a periodic infinite multilayer for three different n_H/n_L ratios. The omnidirectional bandgaps are black colored. We can observe that the structure with ratio n_H/n_L=2.1/1.55 does not have any omnidirectional bandgap. On the contrary, the other two structures have an omnidirectional bandgap.

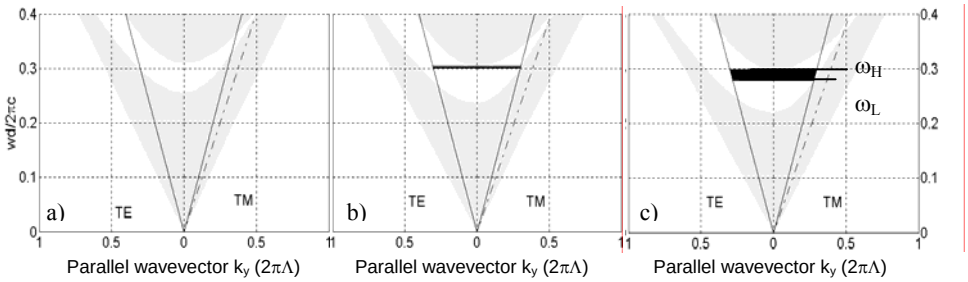

Fig. 4.1. Projected band structure of a multilayer with n_H/n_L=2.1/1.5 (left), n_H/n_L=2.3/1.5 (center) and n_H/n_L=2.5/1.5 (right).

In this figure we can also observe that the refractive indices not only determine the existence of the bandgap but also its width. The omnidirectional bandgap of the structure represented in Fig. 4.1c is wider than the one in Fig. 4.1b. Is the width of the omnidirectional bandgap related to the n_H/n_L ratio? Or there is an optimum n_L for each n_H? Can we calculate the optimum n_H and n_L for obtaining the widest omnidirectional bandgap? The answers to all these questions are given in the two next subsections.

a) Influence of n_H on the width of the omnidirectional bandgap

In this section we study the omnidirectional bandgap width for a given high refractive index layer, n_H. In fact, we study the relative gap width, which is expressed as ($\Delta\omega/\omega_0$)

$$\frac{\Delta\omega}{\omega_0} = \frac{\omega_H - \omega_L}{(1/2)(\omega_H + \omega_L)} \tag{4.1}$$

UNIVERSITAT ROVIRA I VIRGILI
DESIGN, FABRICATION AND CHARACTERIZATION OF POROUS SILICON MULTILAYER OPTICAL DEVICES
Elisabet Xifré Pérez
ISBN: 978-84-691-0362-3/DL: T.2181-2007

where ω_H and ω_L are the upper and lower limits of the omnidirectional bandgap (see Fig. 4.1) and ω_0 is the center frequency of the omnidirectional bandgap.

The influence of n_H on the omnidirectional bandgap width can be observed in Fig. 4.2 that shows the maximum relative band width, $(\Delta\omega/\omega_0)_{max}$ as a function of the high-index value n_H. It is clear from the graph that the maximum value of $(\Delta\omega/\omega_0)$ increases when increasing n_H. It can be observed that the minimum value for n_H to obtain an omnidirectional reflection is 2.25 and that the maximum $(\Delta\omega/\omega_0)$ is around 0.12, which is approximately the maximum attainable $(\Delta\omega/\omega_0)$ using porous silicon.

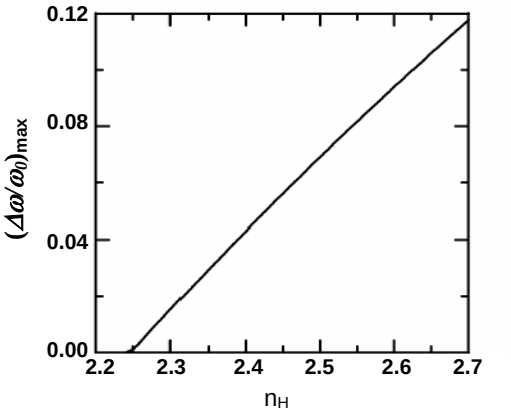

Fig. 4.2. Maximum $(\Delta\omega/\omega_0)$ ratio as a function of the high refractive index (n_H).

b) Influence of n_L on the width of the omnidirectional bandgap

We now analyse the influence of the low refractive index value on the width of the omnidirectional bandgap. From the field of photonic crystals, it is known that the bigger the contrast between the high- and low-refractive indices the wider the photonic bandgap. We have observed in the previous section that the relative gap width increases with increasing n_H until the upper bound for n_H

UNIVERSITAT ROVIRA I VIRGILI
DESIGN, FABRICATION AND CHARACTERIZATION OF POROUS SILICON MULTILAYER OPTICAL DEVICES
Elisabet Xifré Pérez
ISBN: 978-84-691-0362-3/DL: T.2181-2007

(limited by the porous silicon technology) is reached. In this section we evaluate if the complementary hypothesis is right, that is, if the decrease of n_L leads to a increase of the relative gap width.

To this end, we have calculated the relative bandgap width ($\Delta\omega/\omega_0$) that can be attained for every pair (n_H,n_L). The results are plotted in Fig. 4.3a, where ($\Delta\omega/\omega_0$) is represented for every point (n_H,n_L). The points with the same ($\Delta\omega/\omega_0$) are connected obtaining the contours of constant ($\Delta\omega/\omega_0$). The straight line connects the maximum ($\Delta\omega/\omega_0$) for every value of n_H. From this plot we can conclude that there exists an optimal n_L for every n_H, and that for the whole range of n_H this optimal n_L is around 1.5. Fig. 4.3b shows the straight line in Fig. 4.3a with a closer scale so that the variation can be observed in detail.

This fact leads to an important conclusion for porous silicon omnidirectional mirrors: there is no advantage in lowering the low refractive index below this optimal n_L, and therefore the decrease of n_L does not necessary lead to an increase of the relative gap width. Another important conclusion obtained from these results is the difference between the optimal refractive indices for a DBR and for an omnidirectional mirror. For DBR, where the structure is optimised for only one angle of incidence, the widening of the bandgap depends on the ratio n_H/n_L and the higher the ratio the widest the bandgap; whereas for omnidirectional mirrors, the width of the omnidirectional bandgap cannot be studied in terms of n_H/n_L ratio. For the design of an omnidirectional mirror, the most appropriate is to consider both refractive indices separately, as has been done in this section, because an increment of the n_H/n_L ratio, does not necessarily lead to a widening of the omnidirectional bandgap.

UNIVERSITAT ROVIRA I VIRGILI
DESIGN, FABRICATION AND CHARACTERIZATION OF POROUS SILICON MULTILAYER OPTICAL DEVICES
Elisabet Xifré Pérez
ISBN: 978-84-691-0362-3/DL: T.2181-2007

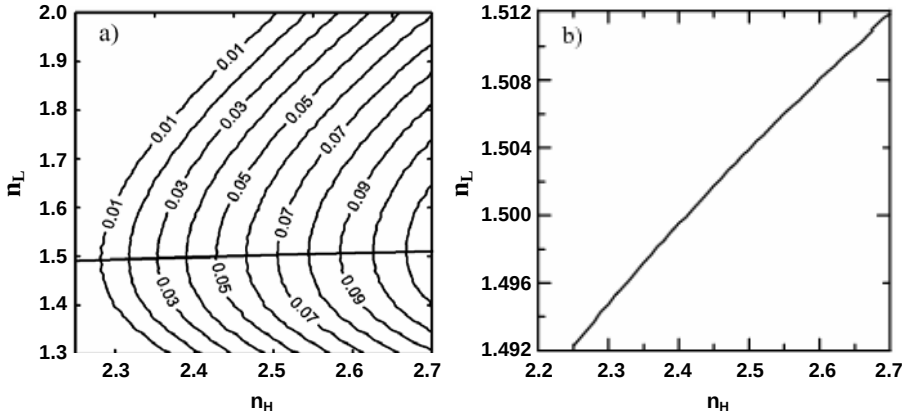

Fig. 4.3. a) Contours of constant ($\Delta\omega/\omega_0$) as a function of the high refractive index n_H and the low refractive index n_L. The straight line connects the points (n_H,n_L) with the $(\Delta\omega/\omega_0)_{max}$ for every value of n_H. b) Zoom of the straight line plotted in a) to show the variation of the optimal n_L.

4.1.1.2. Thickness of one layer (h_H) and period thickness (Λ) ratio: (h_H/Λ)

The first question that arise when designing an omnidirectional mirror, and after the determination of (n_H,n_L), is the optimal value of thickness for the high-index and the low-index layers. It is well accepted that for mirrors for a fixed angle of incidence (with applications in laser resonators, laser optics, imaging systems), the optimal design is the quarter wave stack: a stack where the optical thickness of the layers is a quarter of the design wavelength, taking into account the angle of incidence in the case of non-normal incidence. However, the case here is quite different as there is not a fixed angle of incidence, but the mirror must be high-reflecting for all possible angles and all polarizations for a wavelength range as large as possible.

The bandgap width depends on three variables n_H, n_L and h_H, because h_L depends on h_H with the expression $h_L=\Lambda-h_H$. Therefore we could the relativegap

UNIVERSITAT ROVIRA I VIRGILI
DESIGN, FABRICATION AND CHARACTERIZATION OF POROUS SILICON MULTILAYER OPTICAL DEVICES
Elisabet Xifré Pérez
ISBN: 978-84-691-0362-3/DL: T.2181-2007

width as a function for these variables. But here we study the bandgap as a function of two different variables: the total optical thickness of one period of the photonic crystal, $o_T=n_H \cdot h_H+n_L \cdot h_L$, and the ratio between optical thicknesses $o_R=n_L \cdot h_L/n_H \cdot h_H$. The choice of o_R and o_T for the representation is motivated by the fact that in this way it is easier to recognize the maximum width and its position. Besides, with these two variables it is easier to interpret the results in terms of usual magnitudes in thin-film coating design. In order to be general enough, the optical thicknesses are expressed in terms of the design wavelength.

Fig. 4.4 shows the contours of constant ($\Delta\omega/\omega_0$) as a function of o_T and o_R for three different values of n_H: $n_H=2.30$, $n_H=2.50$, $n_H=2.70$. It is worth reminding that the refractive index of porous silicon may range from 1.2 to 2.7, approximately. The maximum ($\Delta\omega/\omega_0$), its position and its value are indicated in each plot.

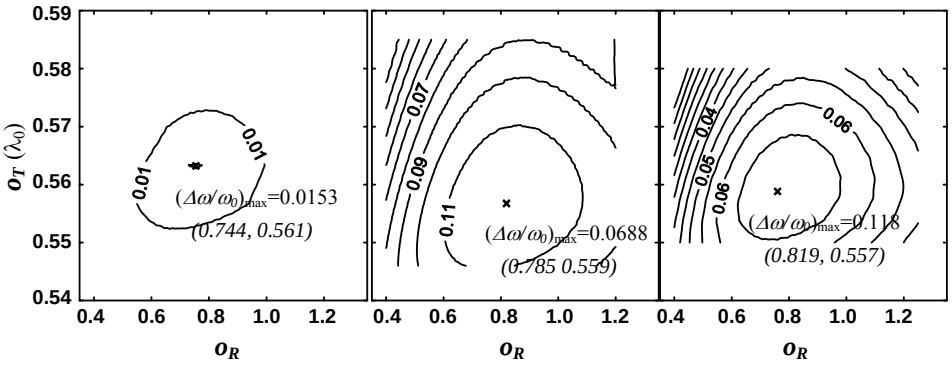

Fig. 4.4. Contours of constant ($\Delta\omega/\omega_0$) for a) n_H =2.3, b) n_H=2.5, c) n_H=2.7. The maximum ($\Delta\omega/\omega_0$) is marked by a cross symbol and its value and the pair (o_R,o_T) for this maximum is written.

In the graphs we can observe that the maximum ($\Delta\omega/\omega_0$) appears approximately at the same position for all the values of n_H. If we observe the results for $n_H=2.50$, this maximum is at $o_R=0.785$ and $o_T= 0.559\lambda_0$, that correspond to optical thicknesses $o_H=n_H \cdot d_H=0.313\lambda_0$ and $o_L=n_L \cdot d_L=0.246\lambda_0$.

UNIVERSITAT ROVIRA I VIRGILI
DESIGN, FABRICATION AND CHARACTERIZATION OF POROUS SILICON MULTILAYER OPTICAL DEVICES
Elisabet Xifré Pérez
ISBN: 978-84-691-0362-3/DL: T.2181-2007

Notice that the total optical thickness o_T is slightly bigger than half of the design wavelength and that the ratio of the optical thicknesses o_R is not 1. Consequently, the quarter-wave design, which gives the maximum width at a given angle of incidence, is not the optimal if all incidence angles are considered.

Now that the quarter-wave structure is known not to be the optimal design, we study the optimal h_H/Λ that leads to the maximum ($\Delta\omega/\omega_0$). In Fig. 4.5, an example case with n_H=2.5 and n_L=1.5 is shown. The PBS of the periodic infinite multilayer for three different values of h_H/Λ are plotted. We can observe that the width of the omnidirectional bandgap depends on the h_H/Λ ratio, and that there is an optimal h_H/Λ ratio for which the omnidirectional bandgap is maximum. Although Fig. 4.5 only shows the simulations for three h_H/Λ values, the simulations have been realized for all the values of h_H/Λ between 0.2 and 0.8, with step 0.01, and it has been observed that the ratio resulting in the widest omnidirectional bandgap is h_H/Λ=0.4. Although the optimal ratio is 0.4 for these n_H and n_L values, each pair (n_H,n_L) that presents an omnidirectional bandgap has its own optimal h_H/Λ, that has to be calculated for every single case.

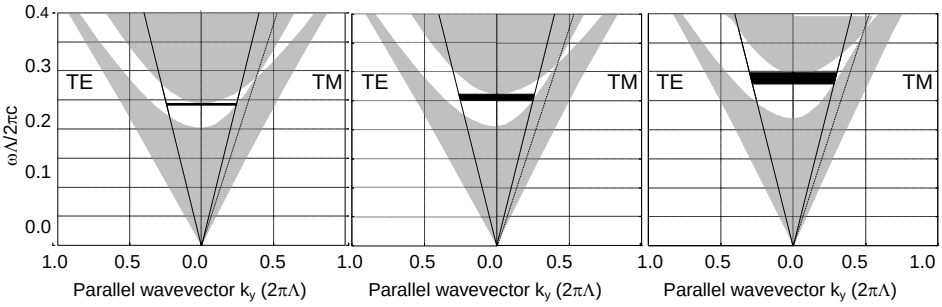

Fig. 4.5. Projected band structure of a multilayer with n_H=2.5, n_L=1.5 for h_H/Λ=0.7 (left), h_H/Λ=0.6 (center) and h_H/Λ=0.4 (right).

UNIVERSITAT ROVIRA I VIRGILI
DESIGN, FABRICATION AND CHARACTERIZATION OF POROUS SILICON MULTILAYER OPTICAL DEVICES
Elisabet Xifré Pérez
ISBN: 978-84-691-0362-3/DL: T.2181-2007

4.1.1.3. Number of periods

The mirrors studied in the previous subsections are infinite periodic structures. These structures are ideal since real multilayers have a finite number of periods N. Although real multilayers have few periods, the reflectivity spectrum of finite multilayers tends to the reflectivity spectrum of infinite multilayers exponentially with N [161] Thus, not many periods of the finite multilayer are needed to obtain bandgap widths similar to the ones calculated from the PBS. When the number of periods N increases, the reflectivity of the bandgap increases and its edges are sharper.

This can be observed in Fig. 4.6 that shows the reflectivity spectrum of a multilayer with n_H=2.5, n_L=1.55 and h_H/Λ=0.4 for different number of periods. The omnidirectional bandgap is defined between the lower band-edge of the normal incidence spectrum and the higher band-edge of the perpendicular incidence spectrum for TM polarization, because this polarization is more restrictive than TE polarization. For N=5, it can be clearly seen that the normal incidence spectrum has a low reflectivity and that, for perpendicular incidence the reflectivity neither reaches the unity for any wavelength within the bandgap. It can be considered that the omnidirectional bandgap does not exist. For N=20, the omnidirectional bandgap exists and is centered at 1.55 μm. It can be also observed that the limits of the omnidirectional bandgap are sharper when N increases.

Up to this point, the influence of the different parameters on the omnidirectional bandgap is known. Now, the optimal parameters to obtain the widest omnidirectional bandgap at λ=1.55 μm with porous silicon are estimated.

UNIVERSITAT ROVIRA I VIRGILI
DESIGN, FABRICATION AND CHARACTERIZATION OF POROUS SILICON MULTILAYER OPTICAL DEVICES
Elisabet Xifré Pérez
ISBN: 978-84-691-0362-3/DL: T.2181-2007

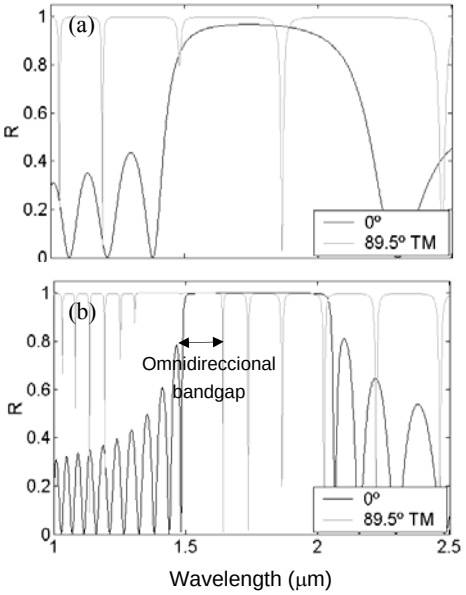

Fig. 4.6. Reflectivity spectrum of a multilayer with n_H=2.5, n_L=1.55 and h_H/Λ=0.4 and number of periods a) N= 5 b) N=20.

4.1.1.4. Omnidireccional mirror with a periodic structure for 1.55 μm applications.

As we have demonstrated in previous sections, the refractive indices *(n_H,n_L)* and the thickness ratio h_H/Λ determine the existence and the width of the omnidirectional bandgap in a periodic multilayer. It has also been observed that the projected band structure of the multilayer shows graphically the width of the omnidirectional bandgap and the normalized frequencies at which it exists.

For the design of the periodic porous silicon mirror for 1.55 μm applications, two typical and obtainable porous silicon refractive indices [19] have been chosen. In the previous sections it has been demonstrated that the higher n_H, the wider the omnidirectional bandgap. For this reason, the high refractive index chosen is 2.5, that is a typical high refractive index for porous silicon. A higher n_H value would imply a high complexity during the fabrication

UNIVERSITAT ROVIRA I VIRGILI
DESIGN, FABRICATION AND CHARACTERIZATION OF POROUS SILICON MULTILAYER OPTICAL DEVICES
Elisabet Xifré Pérez
ISBN: 978-84-691-0362-3/DL: T.2181-2007

process of porous silicon. In the previous section it has been demonstrated that for this n_H, the optimal low refractive index for the widest omnidirectional bandgap is n_L=1.5, when the incidence medium is air. These two refractive indices have been obtained by other authors using the porous silicon technology [39].

The periodic mirror structure obtained with these two refractive indices has an omnidirectional bandgap, whose width depends on the ratio h_H/Λ. The largest omnidirectional bandgap of this structure is obtained when ratio h_H/Λ is 0.4. Fig. 4.7a shows the projected band structure of this infinite periodic multilayer calculated with the transfer matrix method. The central normalized frequency of the omnidirectional bandgap is ω_c=0.2954, and the width is ω_H-ω_L =0.3053-0.2855=0.0198. The central wavelength of the bandgap (λ_c) depends on the period thickness Λ, according to $\omega_c=\Lambda/\lambda_c$. Therefore, the periodic structure with the omnidirectional bandgap centered at 1.55 μm has a $\Lambda=\omega_c.\lambda_c$ = 458 nm. The thickness of the two layers of the period will be h_H=0.4Λ=183 nm and h_L=275 nm.

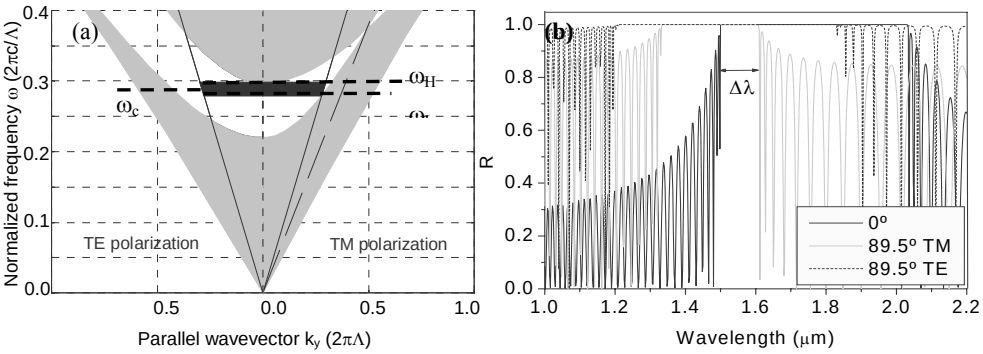

Fig. 4.7. (a) Projected band structure of an infinite periodic multilayer with n_H=2.5, n_L=1.5, h_H/Λ=0.4. The solid lines indicate the light lines and the dashed line indicates the Brewster line. The black area indicates the omnidirectional bandgap. (b) Reflectivity spectrum of a periodic multilayer with 42 periods for TE and TM polarizations and for incidence angles 0º and 89.5º. The width of the omnidirectional bandgap is Δλ=110 nm, centered at 1.55 μm.

UNIVERSITAT ROVIRA I VIRGILI
DESIGN, FABRICATION AND CHARACTERIZATION OF POROUS SILICON MULTILAYER OPTICAL DEVICES
Elisabet Xifré Pérez
ISBN: 978-84-691-0362-3/DL: T.2181-2007

The reflectivity spectrum of this mirror with a finite number of periods (N=42) is shown in Fig. 4.7b. The width of the omnidirectional bandgap is 110 nm for a reflectivity higher that 99%. As can be seen in this figure, the omnidirectional bandgap is centered at 1.55 μm.

Some omnidirectional mirror applications (waveguides [128], antennas substrates [162], etc.) require wide bandgaps. A wide omnidirectional bandgap can be obtained appropriately choosing (n_H,n_L) and its corresponding optimal h_H/Λ, as has been demonstrated in this section. But, as explained before, the maximum refractive index of porous silicon is limited due to the characteristics of the material. Another way for obtaining mirrors with a wider omnidirectional bandgap, keeping constant the refractive indices (n_H,n_L), is modifying the structure of the multilayer. The aim of the multilayer structures that are explained in the next sections is the widening of the omnidirectional bandgap. The omnidirectional bandgap width of all of them will be compared with the one of the periodic mirror structure studied in this section.

4.1.2. Chirped OM

In order to obtain enlarged omnidirectional bandgap mirrors, Yablonovitch [113] proposed the chirped structure. It is a multilayer consisting of N bilayers with refractive index n_H and n_L, where the thickness of the bilayer Λ is continuously increased. In the case of porous silicon, this increment is obtained by increasing the etching time for each layer. Although this structure was firstly proposed by E. Yablonovitch [113] it has been fabricated in porous silicon only by the group of G. Lérondel for 1.3 μm applications [39], demonstrating that chirped structures exhibit an enlarged omnidirectional bandgap.

UNIVERSITAT ROVIRA I VIRGILI
DESIGN, FABRICATION AND CHARACTERIZATION OF POROUS SILICON MULTILAYER OPTICAL DEVICES
Elisabet Xifré Pérez
ISBN: 978-84-691-0362-3/DL: T.2181-2007

4.1.2.1. Omnidirectional mirror with chirped structure for 1.55 μm applications.

For the design and simulation of the chirped structure, the parameters chosen are the ones determined in the periodic OM study. These parameters are n_H=2.5, n_L=1.5 and h_H/Λ=0.4. The use of these same parameters for all the mirror structures studied in this section will enable the comparison between them.

The group of values of Λ in the chirped structure is named bilayers thickness range [Λ], and it determines the wavelength at which the omnidirectional bandgap is centered. By studying the behavior of the chirped structure, a relation between the range [Λ] and the central wavelength of the omnidirectional bandgap (λ_C) has been determined: it can be considered that a chirped structure is a periodic structure with Λ equal to an averaged value of [Λ]. In section 4.1.1.4 the thickness Λ of the periodic structure with these characteristics has been calculated for λ_c=1.55 μm, resulting in Λ= 458 nm. Therefore, the average value of the thickness range [Λ] has to be approximately 458 nm.

Fig. 4.8 shows the reflectivity spectrum of this chirped structure consisting of 42 bilayers where the thickness Λ increases continuously from 381 to 516 nm. The number of bilayers is the same used for the periodic mirror in order to better compare the results with both structures. The omnidirectional bandgap is centered at 1.55 μm and its width for reflectivity higher than 99% is 362 nm.

Notice that the omnidirectional bandgap of the chirped structure is wider than the one of the structure with the same characteristics. This can be observed by comparing the bandgap of the periodic structure in Fig. 4.7b and the one of the chirped structure in Fig. 4.8. Both structures have the same refractive indices, the same h_H/Λ ratio and the same number of periods but the bandgap of the chirped structure is 2.7 times wider than the one of the periodic structure.

UNIVERSITAT ROVIRA I VIRGILI
DESIGN, FABRICATION AND CHARACTERIZATION OF POROUS SILICON MULTILAYER OPTICAL DEVICES
Elisabet Xifré Pérez
ISBN: 978-84-691-0362-3/DL: T.2181-2007

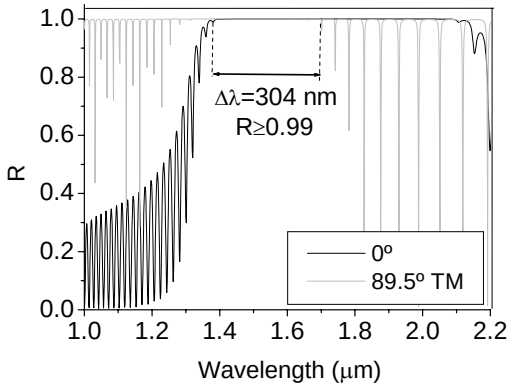

Fig. 4.8. Reflectivity spectrum of the chirped multilayer. The width of the omnidirectional bandgap is 304 nm, centered at 1.55 μm.

4.1.3. Random OM

The multilayers with a random structure were studied for normal incidence by Pavesi [163]. This structure consists of the repetition of two layers with refractive indices n_H (high refractive index layer) and n_L (low refractive index layer). The randomness is obtained as a variation in the thickness of the high refractive index layer (h_H). The set of thicknesses h_H^I is randomly generated, with a histogram that tends to a gaussian distribution centered at the average value $\langle h_H \rangle$ and with standard deviation σ.

Here we study the omnidirectional reflectivity of the random structure. Different parameters of the random multilayer have been studied. All of them have a great influence on the width of the omnidirectional bandgap. Next, these characteristics are explained and discussed:

a) Refractive index of the first layer of the structure.

This layer is in contact with the ambient medium, characterized as n_0 that is usually air. When this first layer is the one with the high refractive index (n_H), the mirror has a wider omnidirectional bandgap than the mirror with the same characteristics where this first layer is the low refractive index layer (n_L).

UNIVERSITAT ROVIRA I VIRGILI
DESIGN, FABRICATION AND CHARACTERIZATION OF POROUS SILICON MULTILAYER OPTICAL DEVICES
Elisabet Xifré Pérez
ISBN: 978-84-691-0362-3/DL: T.2181-2007

Fig. 4.9 shows the reflectivity spectrum of two random mirrors with the same parameters and where the only difference between them lies on this different layer order. It is clearly observable that the bandgap of the first mirror is wider than the one of the second mirror. This effect could be due to the fact that the difference between the refractive indices of air and n_H is higher than the difference between air and n_L [40].

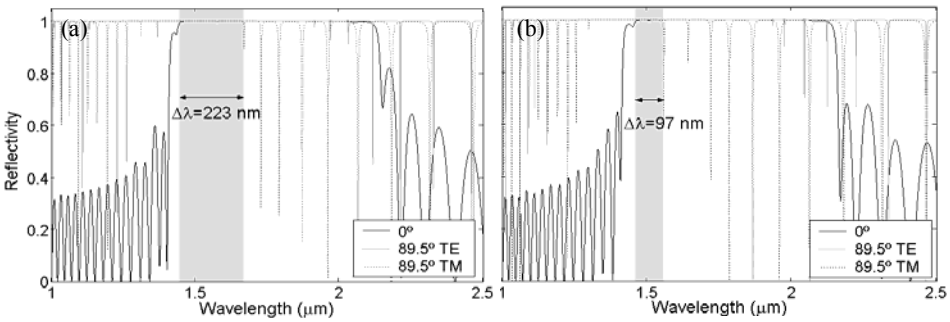

Fig. 4.9. Reflectivity spectrum of two mirrors with n_H=2.5, n_L=1.55, h_L=268 nm and the same h_H^I. The first layer of the mirror is a) n_H and b) n_L. The omnidirectional bandgap of the mirrors is gray colored.

b) Standard deviation

The standard deviation σ of the set of thicknesses h_H^I influences on the width of the bandgap. Fig. 4.10 shows three random structures where the only difference among them is the deviation σ. We can observe that the increase of the deviation σ leads to the widening of the omnidirectional bandgap of the mirror.

UNIVERSITAT ROVIRA I VIRGILI
DESIGN, FABRICATION AND CHARACTERIZATION OF POROUS SILICON MULTILAYER OPTICAL DEVICES
Elisabet Xifré Pérez
ISBN: 978-84-691-0362-3/DL: T.2181-2007

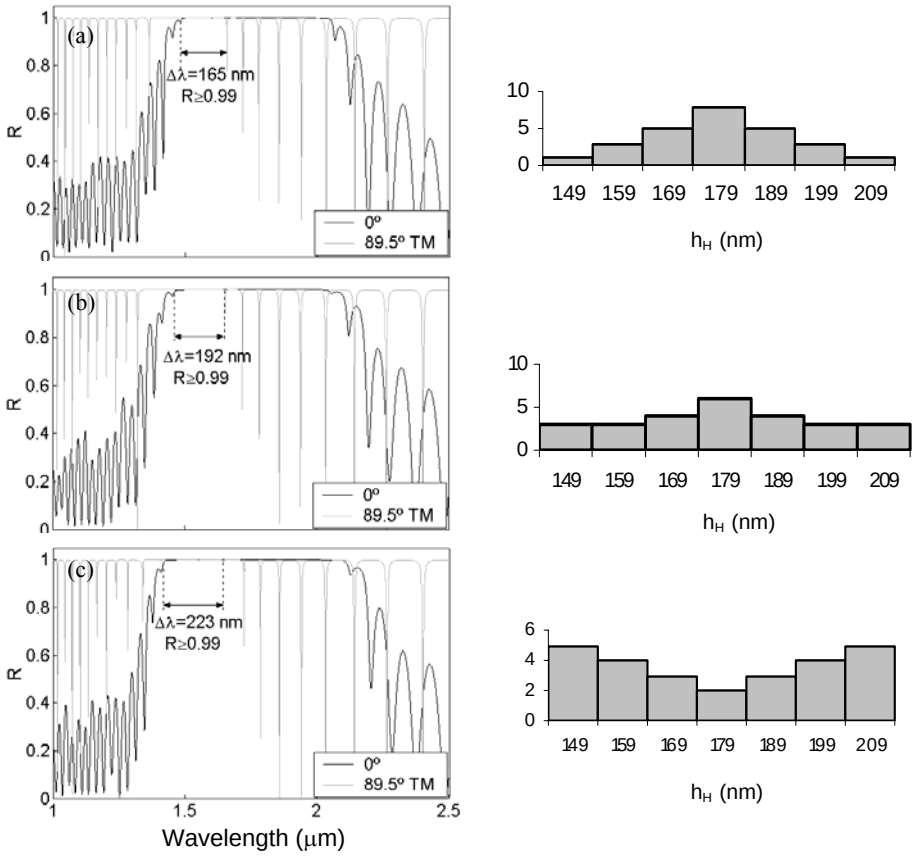

Fig. 4.10. Reflectivity spectrum of random structure mirrors with n_H=2.5, n_L=1.5, h_L=268 nm and 26 periods. The deviation σ of the set of values h_H^I is a) σ=14.14e-9 b) σ=18.19e-9 c) σ=22.19e-9. At the right side of the spectral representation, the histogram with the number of times that each thickness h_H has been used is shown.

c) Average of the set of values h_H^I (<h_H>)

The central wavelength (λ_c) of the omnidirectional bandgap is determined by the average value <h_H>. In fact, the random structure can be considered a periodic structure regarding to the refractive index, and its period Λ can be expressed as Λ=<h_H>+h_L. Using this nomenclature, the projected band

UNIVERSITAT ROVIRA I VIRGILI
DESIGN, FABRICATION AND CHARACTERIZATION OF POROUS SILICON MULTILAYER OPTICAL DEVICES
Elisabet Xifré Pérez
ISBN: 978-84-691-0362-3/DL: T.2181-2007

structure (PBS) is the one of the multilayer with n_H, n_L and ratio $<h_H>/(<h_H>+h_L)$. From the PBS, the normalized central frequency of the omnidirectional bandgap $<\omega_c>$ is obtained. As has been explained before, this frequency is related with λ_c according to $\lambda_c = \Lambda/\omega_c$. By this way, the estimated central wavelength of the random structure can be calculated as $\lambda_c=(<h_H>+h_L)/<\omega_c>$. The value of the calculated λ_c is orientative, it can not be considered an exact value as the average value $<h_H>$ is used.

d) Difference between two consecutive elements h_H^I

The difference between two consecutive thicknesses h_H^I, that can be expressed as $\Delta=h_H^{i+1}-h_H^i$ for i=1..(N-1), also influences on the width of the omnidirectional bandgap. Fig. 4.11 shows the reflectivity spectrum of two random mirrors with the same characteristics and with the same set of thicknesses h_H^I, but in a different order. Whereas for the first mirror Δ is constant or zero, the second has a variable Δ. It can be observed that the omnidirectional bandgap of the second mirror is considerably narrower than the one of the first mirror. We can conclude that the mirrors with the set of thicknesses h_H^I where Δ is constant or zero have a wider omnidirectional bandgap than those where Δ is variable.

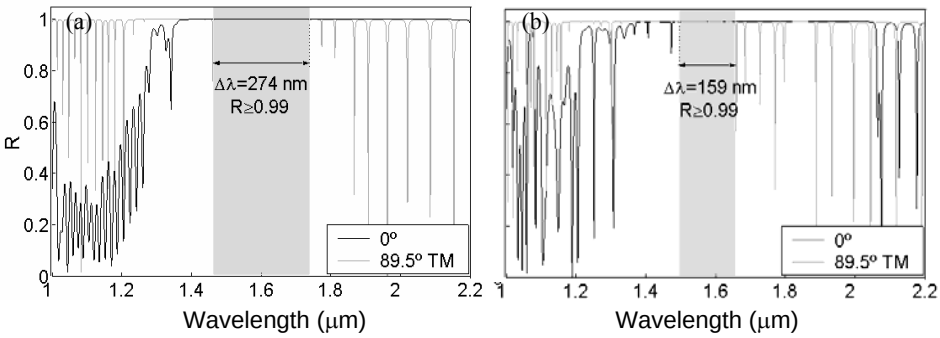

Fig. 4.11. Reflectivity spectrum of two mirrors with n_H=2.5, n_L=1.55, h_L=268 nm and 42 periods. The difference Δ is a) constant or zero, b) variable.

UNIVERSITAT ROVIRA I VIRGILI
DESIGN, FABRICATION AND CHARACTERIZATION OF POROUS SILICON MULTILAYER OPTICAL DEVICES
Elisabet Xifré Pérez
ISBN: 978-84-691-0362-3/DL: T.2181-2007

e) Distribution of the elements h_H^I

The order of the elements in the set h_H^I influences on the width of the omnidirectional bandgap. The elements h_H^I can be increasingly ordered, that is, from low to high thickness, being the lower the one in contact with the air. They could also be decreasingly ordered, or in a random order. Fig. 4.12 shows the reflectivity spectrum of a mirror where the order of the elements h_H^I is different for each case. The multilayer that shows a narrower bandgap is the one with the decreasing order. In the case of the multilayers with random order, it can be clearly seen that the width of the bandgap has a great dependence on the set of elements h_H^I. From these results, we can consider that the mirror with the h_H^I elements decreasingly ordered is the structure that leads to a wide bandgap without the dependence, and therefore, the design complexity of the structure with random series.

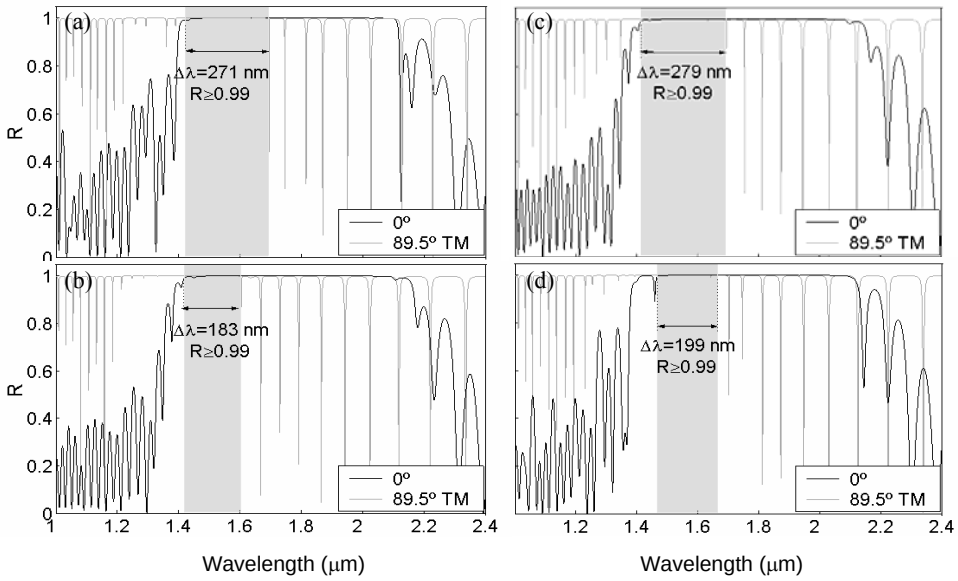

Fig. 4.12. Reflectivity spectrum of the random mirror with n_H=2.5, n_L=1.5, h_L=268 nm, 26 periods and σ=21.56e-9. The order of the elements in h_H^I is a) increasingly ordered, b) decreasingly ordered, c and d) the same set h_H^I but with two different random series. For the four cases Δ is constant or zero.

UNIVERSITAT ROVIRA I VIRGILI
DESIGN, FABRICATION AND CHARACTERIZATION OF POROUS SILICON MULTILAYER OPTICAL DEVICES
Elisabet Xifré Pérez
ISBN: 978-84-691-0362-3/DL: T.2181-2007

4.5.3.1. Random omnidirectional mirror for 1.55 μm applications.

For the design and simulation of the random mirror structure, we have used the same parameters than the ones used for the periodic and chirped structures studied in the previous sections: n_H=2.5, n_L=1.5, h_L=275 nm and N=42 periods. According to the results of the study, the first layer of the structure is the one with n_H.

Considering the similarity between the random and the periodic structure, from the value of ω_c in the projected band structure of the periodic mirror we can calculate the approximate value $<h_H>$ to obtain an omnidirectional bandgap centered at λ_c=1.55 μm. As ω_c=0.2954 (Fig. 4.7a), $<h_H>$ is calculated with $\lambda_c=(<h_H>+h_L)/<\omega_c>$, where λ_c=1.55 μm. For this case, the calculated $<h_H>$ is 183 nm. Therefore, the set h_H^I will consist of 42 elements, where $<h_H>$ will be 183 nm.

The reflectivity spectrum of two random mirrors with these characteristics can be observed in Fig. 4.13a. The distribution of thicknesses h_H^I is random and the difference between two consecutive thicknesses is constant or zero. The average value $<h_H>$ is 183 nm.

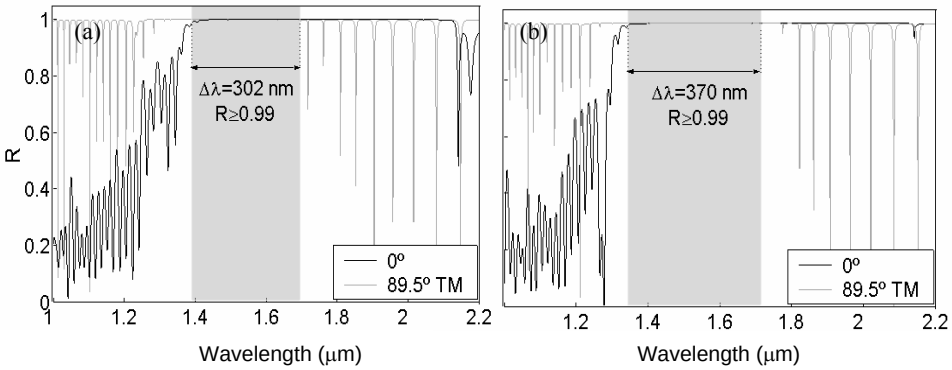

Fig. 4.13. Reflectivity spectrum of two random mirrors with n_H=2.5, n_L=1.5, h_L=275 nm and N=42 periods. The difference Δ is constant. The deviation is a) 23.66e-9 b) 32.38e-9.

UNIVERSITAT ROVIRA I VIRGILI
DESIGN, FABRICATION AND CHARACTERIZATION OF POROUS SILICON MULTILAYER OPTICAL DEVICES
Elisabet Xifré Pérez
ISBN: 978-84-691-0362-3/DL: T.2181-2007

The widest bandgap is obtained for the mirror with highest deviation. Its omnidirectional bandgap is centered at 1.57 μm and its width is 370 nm, 3.4 times the one of the periodic structure. These results agree with the conclusions obtained with the study of the random structure.

4.1.4. New enlarged omnidirectional bandgap mirrors

From the conclusions obtained with the study of the random structure, we have proposed two new omnidirectional mirror structures with enlarged omnidirectional bandgaps. Both mirror structures consist of a few periodic multilayers stacked together, which will be referred to as substructures from now on. Fig. 4.14 shows schematically the substructures that form this type of mirrors. All these substructures have the same refractive indices and the same h_H/Λ ratio. The only difference between them is the thickness period Λ, which is different for every substructure.

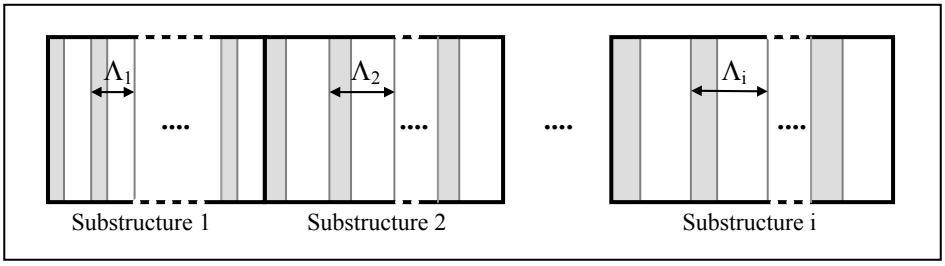

Fig. 4.14. Schematic of the balanced and the unbalanced mirror structures. Both are formed by i substructures with Λ_i and with the same number of periods for the balanced structure and with different number of periods for the unbalanced structure.

The substructures are stacked in order of increasing Λ from the incident medium. The omnidirectional bandgap of the mirror structure is the union of the omnidirectional bandgaps of the substructures that make it up. As has been explained before, the central wavelength of the omnidirectional bandgap is

UNIVERSITAT ROVIRA I VIRGILI
DESIGN, FABRICATION AND CHARACTERIZATION OF POROUS SILICON MULTILAYER OPTICAL DEVICES
Elisabet Xifré Pérez
ISBN: 978-84-691-0362-3/DL: T.2181-2007

determined by Λ. If an appropriate Λ is chosen for every substructure, the bandgaps of adjacent substructures intersect and the resulting mirror will present an enlarged omnidirectional bandgap.

We propose two mirror structures with these characteristics: a balanced mirror structure, where all the substructures that make up the mirror have the same number of periods N, and an unbalanced mirror structure, where the first and the last substructures have more periods than the others.

In order to achieve structures with a wide omnidirectional bandgap, it is important to understand the influence of the parameters characterizing these two new mirror structures. To this end, we consider the bandgap of each substructure separately and their combination. The characterizing parameters of the balanced and the unbalanced mirrors that we propose are:

i) The number of substructures. The width of the omnidirectional bandgap of the mirror is the union of all substructures bandgaps. Consequently, the larger the number of substructures, the wider the omnidirectional bandgap.

ii) The number of periods for each substructure. Since a substructure is not an infinite multilayer, its bandgap is not as wide as the ideal one but slightly narrower. The increment in the number of periods of a substructure leads to the enlargement of its omnidirectional bandgap. We will consider the omnidirectional bandgap of a substructure as the range of wavelengths where the reflectivity spectra is higher than a certain limit R_L for all incidence angles between 0º and 89.5º and for TE and TM polarizations.

iii) The overlap between the omnidirectional bandgaps of adjacent substructures. The smaller the overlap the wider the resulting bandgap. However, this overlap cannot be reduced arbitrarily because the intersection of adjacent bandgaps must result in a reflectivity higher than R_L within the overlapping region.

Taking into account all these parameters, it is clear that to achieve a wide bandgap it is necessary to increase the number of substructures and the

UNIVERSITAT ROVIRA I VIRGILI
DESIGN, FABRICATION AND CHARACTERIZATION OF POROUS SILICON MULTILAYER OPTICAL DEVICES
Elisabet Xifré Pérez
ISBN: 978-84-691-0362-3/DL: T.2181-2007

number of periods per substructure. However, when the total number of periods of the mirror increases, the fabrication complexity increases. If the total number of periods is limited, the first two parameters mentioned above (number of substructures and number of periods of each one) cannot be increased simultaneously and a compromise between them should be found. From this point of view, the periodic and the chirped structures can be considered as extreme configurations: the periodic mirror consisting of a single substructure and the chirped mirror consisting of many single-period substructures. It is expected that, for a fixed total number of periods, a compromise between the number of substructures and the number of periods per substructure could lead to an optimal bandgap width. The two new mirror structures proposed here attempt to meet this compromise.

4.1.4.1. Porous silicon balanced and unbalanced mirrors

In this section, the balanced and the unbalanced mirrors are proposed for applications based on porous silicon technology. To compare the results with the rest of mirror structures, the refractive indices used for the design are n_H=2.5 and n_L=1.5.

Both mirrors, designed here for 1.55 μm applications, are made up of a few periodic multilayer substructures. The number of substructures and their period thicknesses have been chosen as an example to illustrate the concepts introduced previously. The balanced and unbalanced mirrors that we propose are made up of six substructures with period thicknesses chosen as 381, 405, 431, 458, 486 and 516 nm. The first substructure is the one with Λ=381 nm, the second the one with Λ=405 nm and so on, the last one being the substructure with Λ=516 nm. The period thicknesses have been chosen so that the omnidirectional bandgaps overlap and that the omnidirectional bandgap of the resulting mirror is centered at approximately 1.55 μm. The omnidirectional bandgap of each of the six substructures is shown in Fig. 4.15. This figure shows that the omnidirectional bandgaps are adjacent and intersect. The central

UNIVERSITAT ROVIRA I VIRGILI
DESIGN, FABRICATION AND CHARACTERIZATION OF POROUS SILICON MULTILAYER OPTICAL DEVICES
Elisabet Xifré Pérez
ISBN: 978-84-691-0362-3/DL: T.2181-2007

wavelength λ_c and the width of the omnidirectional bandgap increase when Λ increases.

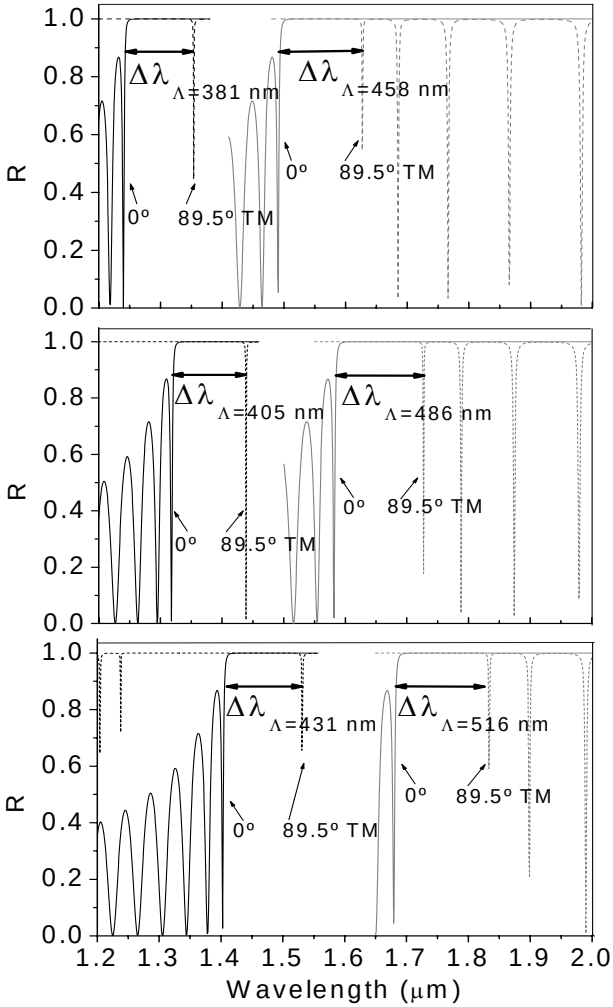

Fig. 4.15. Omnidirectional bandgap of six periodic substructures whose photonic band structure is shown in Fig. 4.7a and with different period thicknesses Λ.

UNIVERSITAT ROVIRA I VIRGILI
DESIGN, FABRICATION AND CHARACTERIZATION OF POROUS SILICON MULTILAYER OPTICAL DEVICES
Elisabet Xifré Pérez
ISBN: 978-84-691-0362-3/DL: T.2181-2007

4.1.4.2. Porous silicon balanced mirror for 1.55 μm applications

The balanced mirror is the one in which all the substructures that make it up have the same number of periods N ($N_1=N_2=...=N_6=N$). We show Table 4.I in order to study the influence of N on the width of the omnidirectional bandgap. The first row indicates the number of periods N of the substructures that make up the balanced mirror. The second row indicates the width of the omnidirectional bandgap for a reflectivity higher than R_L=99%. The third row indicates the total number of periods (N_t) of the balanced mirror. For N<3 the mirror has no omnidirectional bandgap at 1.55 μm. For N≥3, the width of the omnidirectional bandgap increases with N, but the higher N, the smaller the enlargement of the bandgap. As can be seen from the table, a 42-period mirror has a 411 nm omnidirectional bandgap. However, when we double the total number of periods of the balanced mirror (from 42 to 84), the omnidirectional bandgap is only 1.3 times wider. Therefore, the enlargement of the omnidirectional bandgap is not proportional to the N_t increment.

N	3	4	5	6	7	8	9	10	11	12	13	14	15	16
$\Delta\lambda$ (nm)	105	330	386	406	411	428	488	495	497	500	534	535	535	556
N_t	18	24	30	36	42	48	54	60	66	72	78	84	90	96

Table 4.I. Omnidirectional bandgap of the balanced mirror proposed for different number of periods N.

4.1.4.3. Porous silicon unbalanced mirror for 1.55 μm applications

The unbalanced mirror is the one in which the first and the last substructures have more periods than the other substructures. The enlargement of its omnidirectional bandgap can be explained by studying the bandgap of the substructures that make it up. The increase in the number of periods of the

UNIVERSITAT ROVIRA I VIRGILI
DESIGN, FABRICATION AND CHARACTERIZATION OF POROUS SILICON MULTILAYER OPTICAL DEVICES
Elisabet Xifré Pérez
ISBN: 978-84-691-0362-3/DL: T.2181-2007

substructure leads to a wider substructure bandgap and a higher reflectivity. If the bandgap of the first and the last substructures is wider, the bandgap of the resulting mirror will be wider as well. However, the other substructures do not need a high number of periods because their bandgaps overlap.

We have studied many different N_i distributions for the unbalanced mirror. One of these distributions is described in Table 4.II as an example of the unbalanced mirror. The table also shows the parameters of the balanced mirror with the same total number of periods (N_t=42), that are compared with the unbalanced mirror. The reflectivity spectra of the mirrors described in Table 4.II are shown in Fig. 4.16. The omnidirectional bandgap of the balanced mirror, corresponding to a reflectivity higher than 99%, is 411 nm, 3.7 times the periodic mirror bandgap. The one of the unbalanced mirror is 514 nm, 4.7 times the periodic multilayer bandgap. Both are centered at approximately 1.55 μm.

	1st	2nd	3rd	4th	5th	6th
Number of periods N (balanced mirror)	7	7	7	7	7	7
Number of periods N_t (unbalanced mirror)	12	5	4	4	5	12
Period thickness Λ (nm)	381	405	431	458	486	516

Table 4.II. Characteristics of the six substructures that make up the balanced and the unbalanced mirrors for 1.55 μm applications.

UNIVERSITAT ROVIRA I VIRGILI
DESIGN, FABRICATION AND CHARACTERIZATION OF POROUS SILICON MULTILAYER OPTICAL DEVICES
Elisabet Xifré Pérez
ISBN: 978-84-691-0362-3/DL: T.2181-2007

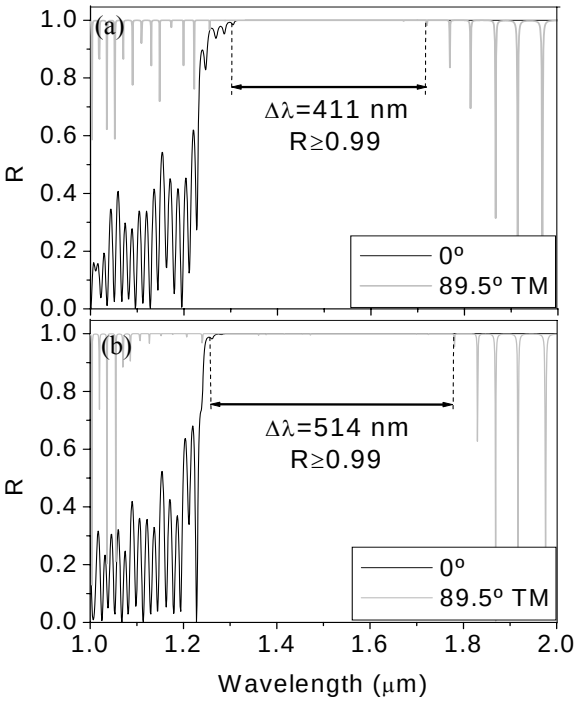

Fig. 4.16. Reflectivity spectra of a) the balanced mirror structure b) the unbalanced mirror structure. Both are centered at 1.55 μm.

4.1.5. Comparison of the studied mirror structures

The results obtained with the balanced and the unbalanced mirrors are compared with the ones obtained with equivalent periodic, chirped and random mirrors. We consider equivalent mirrors those with the same total number of periods, the same refractive indices and centered at 1.55 μm. Furthermore, for the case of the chirped and random mirror, the lower and the higher period thicknesses are the same as those for the proposed balanced and unbalanced mirrors. The bandgaps of these mirrors are summed up in Table 4.III. The omnidirectional bandgap of the periodic mirror with these characteristics is 110 nm, for a reflectivity higher than 99 %. The one of the chirped mirror is 304 nm and 370 nm for the random mirror.

UNIVERSITAT ROVIRA I VIRGILI
DESIGN, FABRICATION AND CHARACTERIZATION OF POROUS SILICON MULTILAYER OPTICAL DEVICES
Elisabet Xifré Pérez
ISBN: 978-84-691-0362-3/DL: T.2181-2007

	Periods	Initial Λ (nm)	Final Λ (nm)	Δλ (R≥0.99) (nm)
Periodic structure	42	458	458	110
Chirped	42	381	516	304
Random	42	391[1]	489[2]	370 (σ=32.38e-9)
Balanced mirror structure, N=(7,7,7,7,7,7)	42	381	516	411
Unbalanced mirror structure, N=(12,5,4,4,5,12)	42	381	516	514

[1]Λ minimum ; [2]Λ maximum

Table 4.III. Comparison of the omnidirectional bandgap of the five mirror structures studied.

We can observe that the unbalanced is the mirror with the widest omnidirectional bandgap, 4.7 times that of the periodic mirror, the optimal for the fabrication of omnidirectional mirrors. The balanced structure also has an enlarged omnidirectional bandgap, concretely 3.7 times the periodic mirror bandgap. The next widest bandgap is the one of the random mirror but this width strongly depends on the order of the thicknesses h_H^I. Finally, the chirped structure is the one with the lower widening, althought its bandgap is 2.7 times greater than the one of the periodic mirror.

The balanced and the unbalanced mirrors have the same number of periods, the same refractive indices and the same range or period thicknesses as the periodic, chirped and random structures. Therefore, the balanced and the unbalanced mirrors have the same technology requirements as the rest of the mirror structures having a widest omnidirectional bandgap.

UNIVERSITAT ROVIRA I VIRGILI
DESIGN, FABRICATION AND CHARACTERIZATION OF POROUS SILICON MULTILAYER OPTICAL DEVICES
Elisabet Xifré Pérez
ISBN: 978-84-691-0362-3/DL: T.2181-2007

4.2. Waveguides

Waveguide structures are important components in optoelectronics and telecommunication systems. Traditionally, light has been confined in waveguides by total internal reflection [125], due to the contrast of the refractive indices of the cladding and the core layers, or by metal cladding, due to the high reflection of a near-perfect metal [164]. A novel class of waveguides has been introduced recently, in which the confinement of the light is based on the properties of photonic crystals. The photonic bandgap, in which light cannot propagate in a certain frequency range, is used to confine light.

In the next sections we present the design of waveguide structures based on porous silicon multilayers, both based on total internal reflection and on photonic crystals. We investigate the necessary conditions for the existence of modes and the influence of the dimensions and refractive indices of the layers on the properties of the waveguide.

4.2.1. Total internal reflection waveguides

The most commonly used waveguide structures are the ones based on the total internal reflection effect (TIR). These dielectric slab waveguides consist of a core layer inserted in between two layers, named cladding. The refractive index of the core is higher than the refractive index of the cladding layers. We propose a symmetric planar dielectric waveguide made of a core with thickness d and refractive index n_1 surrounded by a cladding of smaller refractive index n_2, as illustrated in Fig. 4.17.

UNIVERSITAT ROVIRA I VIRGILI
DESIGN, FABRICATION AND CHARACTERIZATION OF POROUS SILICON MULTILAYER OPTICAL DEVICES
Elisabet Xifré Pérez
ISBN: 978-84-691-0362-3/DL: T.2181-2007

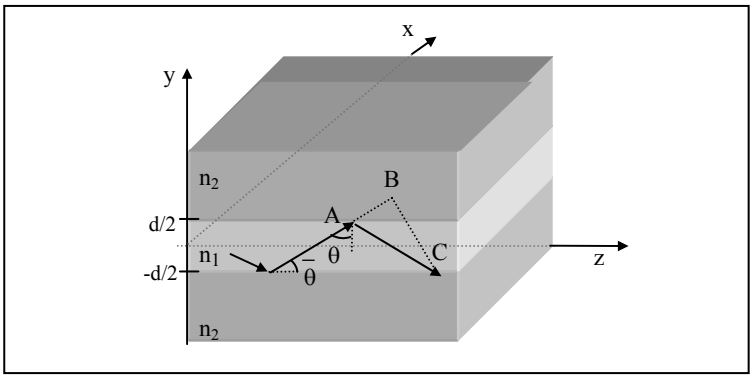

Fig. 4.17. Schematic of the multilayer waveguide consisting of three layers. The inner layer, with refractive index n_1, is the core of the waveguide. The outer layers are the cladding and their refractive index is n_2, that is lower than n_1. Rays making an angle $\theta>\theta_c$ are guided by total internal reflection.

4.2.1.1. Total internal reflection principles

Light rays making angles θ, measured from the normal to the interface, travel along the guiding layer if θ is greater than the critical angle θ_c. The critical angle is expressed as $\theta_c=\sin^{-1}(n_2/n_1)$. These light rays are totally internally reflected at the core/cladding boundary. When θ is smaller than θ_c, the light rays are refracted into the cladding and attenuated.

The waveguide modes can be determined by developing solutions to the Maxwell's equations in the inner and outer media with the appropriate boundary conditions imposed. In order to easily determine these modes, we will write the solution in terms of TEM plane waves bouncing between the surfaces of the slab.

We assume that the field in the slab is in the form of a monochromatic TEM plane wave. The wave travels with a phase velocity $c_1=c_0/n_1$, at a wavelength $\lambda=\lambda_0/n_1$. Its wave number is n_1k_0, and the wavevector components are $k_x=0$, $k_y=n_1k_0 \sin\bar{\theta}$, and $k_z=n_1k_0 \cos\bar{\theta}$, where $\bar{\theta}$ is the complement of the angle θ. In order to determine the modes of the waveguide, the self-consistency

UNIVERSITAT ROVIRA I VIRGILI
DESIGN, FABRICATION AND CHARACTERIZATION OF POROUS SILICON MULTILAYER OPTICAL DEVICES
Elisabet Xifré Pérez
ISBN: 978-84-691-0362-3/DL: T.2181-2007

condition is imposed. According to that condition, a wave reproduces itself after each round trip [165].

In one round trip, the twice-reflected wave lags behind the original wave by a distance $\overline{AC} - \overline{AB} = 2d \sin\bar{\theta}$, as in Fig. 4.17. Each internal reflection at the dielectric boundary introduces a phase φ_r. For self-consistency, the phase shift between the two waves must be zero or multiple of 2π,

$$\frac{2\pi}{\lambda} 2d \sin\bar{\theta} - 2\varphi_r = 2\pi m \qquad \text{m=0,1,2,..} \tag{4.2}$$

Equation (4.2) can be expressed as

$$2k_y d - 2\varphi_r = 2\pi m \tag{4.3}$$

The reflection phase shift φ_r is a function of the angle θ. It also depends on the polarization of the incident wave, TE or TM. In the TE case (the electric field is perpendicular to the plane y-z), the phase shift can be expressed as

$$\tan\frac{\varphi_r}{2} = \left(\frac{\sin^2\theta - \sin^2\theta_c}{\cos^2\theta} \right)^{1/2} \tag{4.4}$$

The dependence of the propagation constant β on the frequency ω can be examined by writing the self-consistency Eq. (4.3) in terms of β and ω. Since $\beta = k_z$ and $k_y^2 = (\omega/c_1)^2 - \beta^2$, Eq (4.3) gives,

$$2d\left[\left(\frac{\omega}{c_1} \right)^2 - \beta^2 \right]^{1/2} = 2\varphi_r + 2\pi m \tag{4.5}$$

Since $\sin\theta = \beta/(\omega/c_1)$ and $\sin\theta_c = n_2/n_1 = c_1/c_2$, Eq. (4.4) becomes

$$\tan^2\frac{\varphi_r}{2} = \frac{\beta^2 - \omega^2/c_2^2}{\omega^2/c_1^2 - \beta^2} \tag{4.6}$$

Substituting (4.6) into (4.5) we obtain the self-consistency condition

UNIVERSITAT ROVIRA I VIRGILI
DESIGN, FABRICATION AND CHARACTERIZATION OF POROUS SILICON MULTILAYER OPTICAL DEVICES
Elisabet Xifré Pérez
ISBN: 978-84-691-0362-3/DL: T.2181-2007

$$\tan^2\left\{\frac{d}{2}\left[\left(\frac{\omega}{c_1}\right)^2-\beta^2\right]^{1/2}-\frac{m\pi}{2}\right\}=\frac{\beta^2-\omega^2/c_2^2}{\omega^2/c_1^2-\beta^2} \tag{4.7}$$

The self-consistency condition establishes a relation between β and ω, the dispersion relation for the different modes m=0,1,... .

The number of TE modes supported by this multilayer dielectric waveguide is the smallest integer greater than

$$M \doteq 2\frac{d}{\lambda_0}NA \tag{4.8}$$

The symbol $\doteq$ denotes that $2d\ NA/\lambda_0$ is increased to the nearest integer. For example, if $2d\ NA/\lambda_0$ =0.9, 1 or 1.1, the number of modes *M* is 1, 2, and 2, respectively. *NA* is the numerical aperture, expressed as

$$NA=\left(n_1^2-n_2^2\right)^{1/2} \tag{4.9}$$

For a fixed wavelength, the number of modes depends on the core thickness *d* and the difference between the refractive indices n_1 and n_2. The higher the thickness or the higher the difference between the refractive indices, the higher the number of TE modes of the waveguide.

In a dielectric waveguide, there is at least one TE mode, since the fundamental mode (m=0) is allowed for any wavelength [166]. However, the higher modes (m=1,2,...) have their own cutoff wavelength (λ_{cm}). It corresponds to the cutoff frequency $(\omega/c)_{cm}$, where $(\omega/c)_{cm}=2\pi/\lambda_{cm}$, that is the lowest frequency that can be guided by the structure for the m mode.

The waveguide with one allowed mode is called single-mode waveguide. This occurs when the slab is sufficiently thin for a fixed frequency.

UNIVERSITAT ROVIRA I VIRGILI
DESIGN, FABRICATION AND CHARACTERIZATION OF POROUS SILICON MULTILAYER OPTICAL DEVICES
Elisabet Xifré Pérez
ISBN: 978-84-691-0362-3/DL: T.2181-2007

4.2.1.2. Porous silicon slab waveguides for 1.55 μm applications

Two typical porous silicon refractive indices have been chosen for the theoretical study of this symmetric waveguide. The core consists of a porous silicon layer with refractive index n_1=2.5. The refractive index of the two cladding layers is n_2=1.5. These are two typical and obtainable porous silicon refractive indices [39].

The numerical aperture is determined by the refractive indices n_1 and n_2. For the refractive indices chosen, the numerical aperture is 2, calculated using Eq. (4.9). According to Eq. (4.8), for a fixed λ_0=1.55 μm, the number of TE modes *M* only depends on the core thickness *d*. From this equation, we obtain that for *d*<387.5 nm only one confined mode is allowed, and the waveguide is called single-mode. When thickness *d* increases, the number of TE modes increases. This effect can be observed in Fig. 4.18, that shows the dispersion relation of this waveguide for different thickness *d*. If we focus our attention for λ_0=1.55 μm ($\omega/c=4.05\cdot10^6$ rad/m), we can see that there is only one mode allowed for *d*=300 nm, there are two modes allowed for *d*=600 nm, three modes for *d*=900 nm, and four modes allowed for *d*=1300 nm, as was expected from the mathematical calculations of *M*.

For a fixed thickness *d*, the number of modes allowed depends on the wavelength. We can observe that all the waveguides presented in Fig. 4.18 have at least one mode of propagation (m=0) for any wavelength. The rest of the modes have a cutoff wavelength λ_{cm} (or cutoff frequency $(\omega/c)_{cm}$) that is the largest wavelength at which a mode is allowed. Fig. 4.18b shows the dispersion relation for *d*=600 nm. We can observe that the fundamental mode is allowed for any wavelength. The first mode (m=1) is allowed for wavelengths lower than approximately 2.6 μm (ω/c higher than $2.4\cdot10^6$ rad/m) and the second mode (m=2) is allowed for wavelengths lower than 1.2 μm (ω/c higher than $5.23\cdot10^6$ rad/m).

UNIVERSITAT ROVIRA I VIRGILI
DESIGN, FABRICATION AND CHARACTERIZATION OF POROUS SILICON MULTILAYER OPTICAL DEVICES
Elisabet Xifré Pérez
ISBN: 978-84-691-0362-3/DL: T.2181-2007

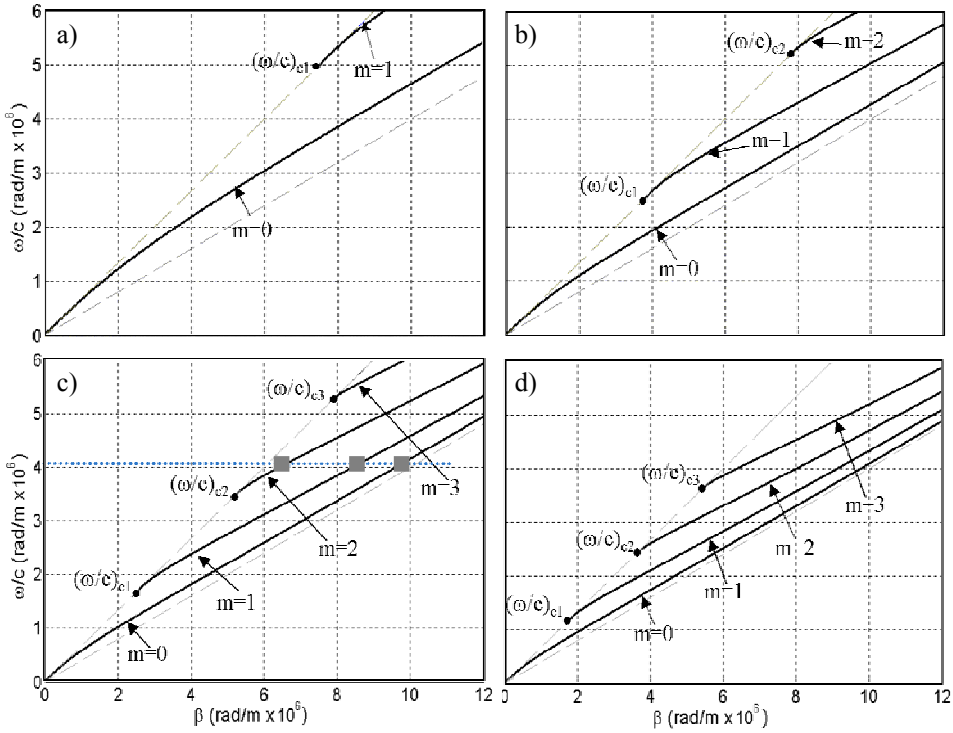

Fig. 4.18. Dispersion relation of the slab waveguide with n_1=2.5, n_2=1.5 and core thickness a) *d*=300 nm b) *d*=600 nm c) *d*=900 nm d) *d*=1300 nm. The modes of the waveguide take place for $n_2<\beta/(\omega/c)<n_1$. The dashed gray lines indicate these two limits. In c) the three modes for λ_0=1.55 μm ($\omega/c=4.05\cdot10^6$ rad/m) are denoted with squares.

We can also study the intensity distribution of all the modes that exist in the waveguide for a certain wavelength. If we focus our attention on the waveguide with *d*=900 nm, and we determine our working wavelength at λ_0=1.55 μm ($\omega/c=4.05\cdot10^6$ rad/m), we can observe in Fig. 4.18c that this waveguide has three different modes, each one for a different β value. The intensity distribution for these three modes is shown in Fig. 4.19. We can observe that all of them are well confined in the core layer, although mode 2 has a small part of the intensity within the cladding layer. All these modes could be

UNIVERSITAT ROVIRA I VIRGILI
DESIGN, FABRICATION AND CHARACTERIZATION OF POROUS SILICON MULTILAYER OPTICAL DEVICES
Elisabet Xifré Pérez
ISBN: 978-84-691-0362-3/DL: T.2181-2007

correctly transmitted through this porous silicon waveguide. The number of modes and the β at which they exist, for a certain wavelength, depends on the thickness of the core *d*, therefore, we could select these parameters adjusting the thickness *d*.

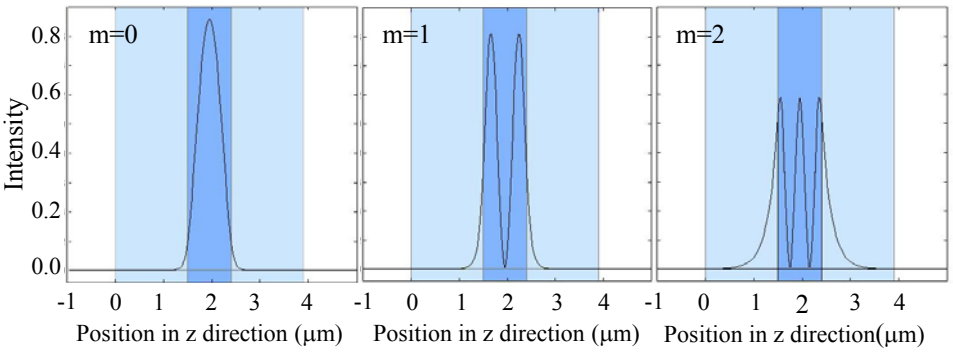

Fig. 4.19. Intensity distribution for the three modes of the waveguide with *d*=900 nm at λ_0=1.55 μm. The wavelength structure is also depicted being the dark gray region the core and the light gray regions the cladding.

Variation of the refractive indices of core and cladding

As explained before, the porous silicon formation technique permits the controlled variation of the refractive indices n_1 and n_2. We now study the influence of the refractive index variation on the cutoff wavelengths of the symmetric waveguides presented. Table 4.IV and Table 4.V show the cutoff wavelength of modes one, two and three for waveguides with core thickness *d* equal to 600 and 900 nm, respectively.

In both tables, we can observe that the variation of one or both refractive indices leads to a variation of the numerical aperture, and therefore a variation of the cutoff wavelengths. The decrease of n_1 and/or the increase of n_2 results in a lower numerical aperture, which leads to lower cutoff wavelengths for all modes.

UNIVERSITAT ROVIRA I VIRGILI
DESIGN, FABRICATION AND CHARACTERIZATION OF POROUS SILICON MULTILAYER OPTICAL DEVICES
Elisabet Xifré Pérez
ISBN: 978-84-691-0362-3/DL: T.2181-2007

n_1	n_2	NA	λ_{c1} (nm)	λ_{c2} (nm)	λ_{c3} (nm)
2.5	1.5	2	2400	1200	800
2.5	1.7	1.83	2196	1098	732
2.5	1.9	1.62	1944	972	648
2.3	1.5	1.74	2088	1044	696
2.1	1.5	1.47	1764	882	588
1.9	1.5	1.17	1404	702	462
2.35	1.7	1.62	1944	972	648

Table 4.IV. Cutoff wavelength of modes m=1...3 for core thickness *d*=600 nm and for different refractive indices n_1 and n_2.

n_1	n_2	NA	λ_{c1} (nm)	λ_{c2} (nm)	λ_{c3} (nm)
2.5	1.5	2	3600	1800	1200
2.5	1.7	1.83	3294	1647	1098
2.5	1.9	1.62	2916	1458	972
2.3	1.5	1.74	3132	1566	1044
2.1	1.5	1.47	2646	1323	882
1.9	1.5	1.17	2106	1053	702
2.35	1.7	1.62	2916	1458	972

Table 4.V. Cutoff wavelength of modes m=1..3 for core thickness *d*=900 nm and for different refractive indices n_1 and n_2.

In both tables, we can observe that, for a fixed *d*, the cutoff wavelength only depends on the resulting numerical aperture and that two waveguides with different refractive indices but with the same *NA* (e.g. *NA*=1.62) have the same cutoff wavelengths.

UNIVERSITAT ROVIRA I VIRGILI
DESIGN, FABRICATION AND CHARACTERIZATION OF POROUS SILICON MULTILAYER OPTICAL DEVICES
Elisabet Xifré Pérez
ISBN: 978-84-691-0362-3/DL: T.2181-2007

4.2.2. Photonic crystal waveguides

A novel class of waveguides has been introduced recently, in which the confinement of the light is based on the properties of photonic crystals (PC). The photonic bandgap, where light cannot propagate for a certain frequency range, is used to confine light.

One-dimensional photonic crystals are multilayer periodic structures that have already been used to confine light in the core layer. Some of them are Distributed Bragg Reflectors (DBR) either in cylindrical [167] or planar structures [125,128]. Others are omnidirectional mirrors (OM) [116,110-112,168,169] that reflect light for any incidence angle and any polarization over a range of frequencies, the so-called omnidirectional bandgap (OBG). We shall focus our attention on planar waveguide structures with OM [170] although cylindrical structures have also been studied [171,172].

4.2.2.1. Structure

The proposed waveguide structure is a porous silicon multilayer consisting of a core layer inserted between two symmetric OM. Fig. 4.20 represents the diagram of this waveguide structure. Each OM is a stack of alternating high and low refractive index layers (n_H and n_L) with thickness d_H and d_L respectively. The period of the OM is defined as $\Lambda=d_H+d_L$ and is repeated N times. The refractive index of the core layer is n_0 and its thickness is d_0.

The refractive indices chosen for the OM are $n_H=2.5$ and $n_L=1.5$ [152]. The number of periods N of the OM should be high enough for the intensity of the electric field (electromagnetic field) of the modes to decay in the OM cladding. The parameter d_H determines the width of the OBG whereas n_0 has an effect on the energy confinement of the modes within the core layer. The optimal values of these three parameters and the criteria for selecting their optimal values are discussed in the next section.

UNIVERSITAT ROVIRA I VIRGILI
DESIGN, FABRICATION AND CHARACTERIZATION OF POROUS SILICON MULTILAYER OPTICAL DEVICES
Elisabet Xifré Pérez
ISBN: 978-84-691-0362-3/DL: T.2181-2007

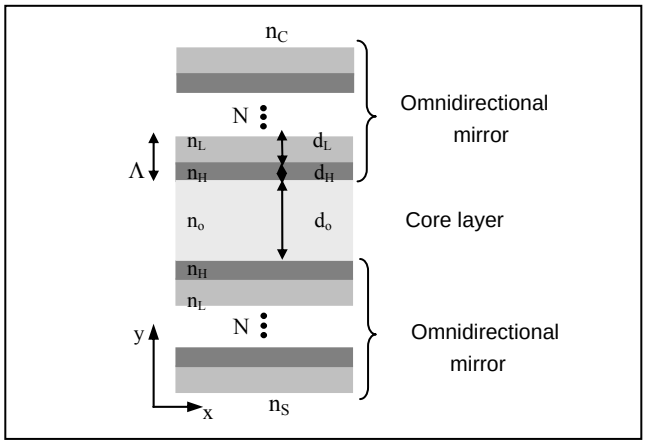

Fig. 4.20. Diagram of the porous silicon multilayer waveguide. n_0 and d_0 are the refractive index and thickness of the core layer, respectively. n_L and n_H are the low and high refractive indices of the omnidirectional mirror cladding layers, while d_L and d_H are their corresponding thicknesses. Each omnidirectional mirror has N periods with period thickness Λ and are surrounded by a cover and a substrate with refractive indices n_C and n_S, respectively. The propagation direction is along the x-axis.

4.2.2.2. Determination of the parameters n_0, d_H and N

In order to study how all the parameters of the structure affect the performance of the waveguide, we applied the transfer matrix method to planar multilayer optical waveguides [156], and restricted our discussion to TE modes. This method is especially suitable for analyzing one-dimensional photonic crystals such as the proposed structure.

Since photonic crystals are perfectly scalable structures, the units of all the magnitudes considered here (thickness, frequency and wavevector) are normalized to the period thickness of the OM (Λ). Thus, to apply the results of this study to a certain frequency, it is only necessary to adjust the period thickness Λ.

UNIVERSITAT ROVIRA I VIRGILI
DESIGN, FABRICATION AND CHARACTERIZATION OF POROUS SILICON MULTILAYER OPTICAL DEVICES
Elisabet Xifré Pérez
ISBN: 978-84-691-0362-3/DL: T.2181-2007

a) Determination of the refractive index of the core layer

The structure that we propose is completely made of porous silicon. Therefore the refractive index of the core layer n_0 could be any refractive index obtainable with the porous silicon fabrication techniques. The core is a porous silicon layer instead of the air layer proposed in previous studies [40,9,43,44]. A porous silicon core ensures the feasibility of the waveguide structure since it can be fabricated in a single etching process by appropriately modulating the etching current. Furthermore, although the core refractive index is higher than 1, it does not negatively affect the properties of the structure [173]; it only slightly reduces the width of the OBG.

The selection criterion used for n_0 is the energy confinement factor of the modes. The confinement (Γ) indicates the portion of the field energy that is confined within the core layer [40] and is defined as:

$$\Gamma = \frac{\int_{Core\ layer} |n_o E|^2 dy}{\int_{-\infty}^{\infty} |n_i E|^2 dy} \tag{4.10}$$

where n_i is the refractive index of the layer for that *y* and *E* is the electrical field amplitude.

Fig. 4.21 shows the confinement of the fundamental mode as a function of n_0 for the range of refractive indices obtainable with porous silicon. The simulated structure is the one presented in the section above and the calculation has been made for three different d_H/Λ so as to consider different possible structures. For the three cases, we can observe that when $n_0>n_L$ the confinement of the mode decreases very quickly with n_0 until the mode disappears. On the other hand, for $n_0 \leq n_L$, the confinement is very similar for the different values of n_0 and the different core thicknesses. This, together with the experimental observation that the fabrication of porous silicon is increasingly more complex when the refractive indices are smaller lead us to choose $n_0=n_L$.

UNIVERSITAT ROVIRA I VIRGILI
DESIGN, FABRICATION AND CHARACTERIZATION OF POROUS SILICON MULTILAYER OPTICAL DEVICES
Elisabet Xifré Pérez
ISBN: 978-84-691-0362-3/DL: T.2181-2007

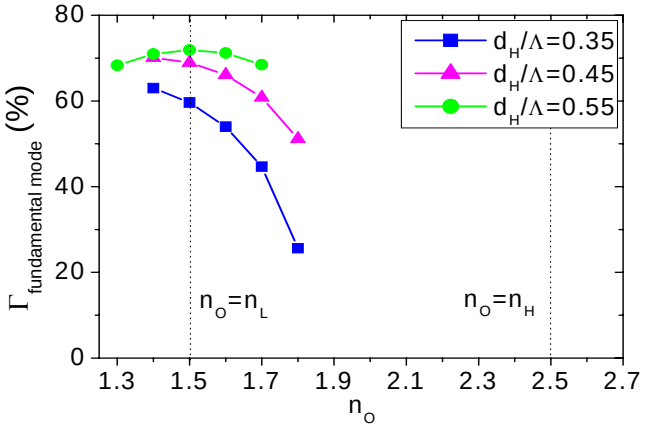

Fig. 4.21. Confinement of the fundamental mode as a function of n_0 in the range of refractive indices obtainable with the porous silicon formation technique. The confinement is calculated for different d_H/Λ and for $\omega(\Lambda/2\pi c)$=0.29 and d_0/Λ=2. We can observe that for $n_0 \geq 1.9$ the fundamental mode does not exist and for n_0=1.3 it does not exist for some d_H/Λ.

b) Determination of the layer thickness of the OM

Selecting the thickness of the OM layers can be reduced to selecting d_H/Λ because $1= d_H/\Lambda + d_L/\Lambda$. The ratio d_H/Λ is an important parameter of the OM because it determines the width of its OBG. The projected band structure (PBS) of the multilayer can be used to easily observe the width of the OBG. Fig. 4.22 shows the PBS for TE polarization of the infinite multilayer with $n_0=n_L$=1.5 and n_H =2.5 for different d_H/Λ. An electromagnetic mode is defined by the frequency ω and the surface-parallel wavevector β, which are expressed in the figure in normalized units. The gray regions represent the allowed modes, the white region over the light line for n_0 represents the bandgap and the black region indicates the OBG. In Fig. 4.22 we can observe that the position and width of the bandgap varies with the thickness d_H/Λ and that the OBG only exists for $0.32 \leq d_H/\Lambda \leq 0.62$. For this study d_H/Λ was taken to satisfy the widest OBG condition, which corresponds to d_H/Λ=0.45.

UNIVERSITAT ROVIRA I VIRGILI
DESIGN, FABRICATION AND CHARACTERIZATION OF POROUS SILICON MULTILAYER OPTICAL DEVICES
Elisabet Xifré Pérez
ISBN: 978-84-691-0362-3/DL: T.2181-2007

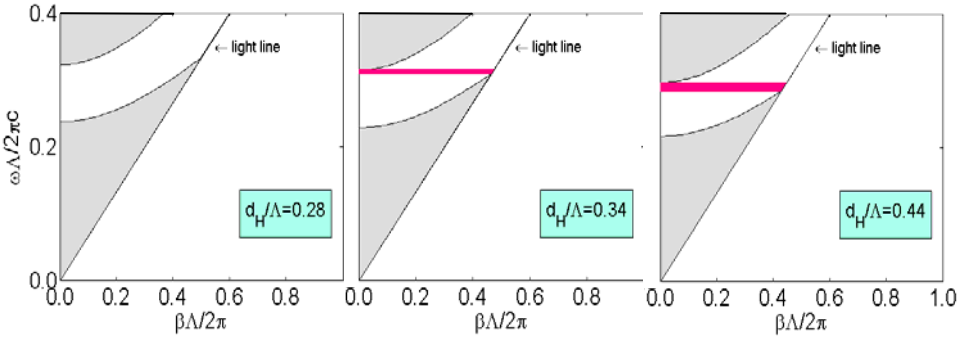

Fig. 4.22. Projected band structure of the mirror cladding with n_H=2.5 and n_L=1.5, for different d_H/Λ. The *x* axis corresponds to the normalized surface-parallel wavevector component β and the *y* axis is the normalized frequency ω. The thin black line is the light line for n_0=1.5. The black area is the OBG, which only exists for $0.32 \leq d_H/\Lambda \leq 0.62$.

c) Determination of the OM number of periods

The number of periods (N) affects the OM because the more there are, the more similar the behavior of the finite OM is to the ideal infinite photonic crystal. The field of a mode with (ω,β) in the bandgap of the OM is guided in the core layer and is attenuated as it penetrates the periods of the OM.

This effect can be observed in Fig. 4.23 where the field profiles of the three existing guided modes for d_0/Λ=6 and normalized frequency $\omega(\Lambda/2\pi c)$=0.29 are represented together with 15-period OM claddings. The field is highly confined within the core layer for all the guided modes while the field amplitude becomes attenuated as it penetrates the cladding. In this study, the criterion for determining N was the attenuation of the field amplitude in the cladding. In particular, the chosen N is the one that leads to an attenuation of 100 dB from the maximum in the core to the outermost period of the OM for the higher order mode. For the refractive indices and thicknesses determined above, the number of periods that fulfills this condition is N=15, for any core thickness.

UNIVERSITAT ROVIRA I VIRGILI
DESIGN, FABRICATION AND CHARACTERIZATION OF POROUS SILICON MULTILAYER OPTICAL DEVICES
Elisabet Xifré Pérez
ISBN: 978-84-691-0362-3/DL: T.2181-2007

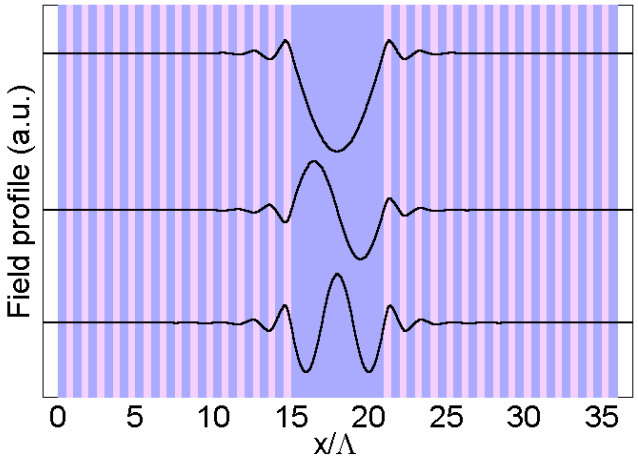

Fig. 4.23. Field profile of the guided modes in the proposed structure. The multilayer structure for 15 periods is depicted and the three modes for $d_0/\Lambda=6$ and $\omega(\Lambda/2\pi c) =0.29$ are superposed.

4.2.2.3. Omnidirectional Mirrors and Distributed Bragg Reflectors as cladding for porous silicon planar waveguides

Once the omnidirectional mirror parameters (n_H, n_L, d_H and N) and the refractive index of the core layer (n_0) have been determined, we can evaluate the use of the OM as cladding in planar waveguides. To this end, we will study how the core thickness influences on the number of guided modes and their confinement, and also the dependence of the confinement of the modes on frequency.

a) Influence of the core thickness

The number of guided modes and their confinement are determined by the core thickness d_0. Fig. 4.24 shows the dispersion relation for the modes for different core thicknesses d_0/Λ together with the PBS of the OM. Notice that the

UNIVERSITAT ROVIRA I VIRGILI
DESIGN, FABRICATION AND CHARACTERIZATION OF POROUS SILICON MULTILAYER OPTICAL DEVICES
Elisabet Xifré Pérez
ISBN: 978-84-691-0362-3/DL: T.2181-2007

PBS is the same for any d_0/Λ because the characteristics of the OM are independent of this parameter. When d_0/Λ is very low there is only one mode, the fundamental or first mode. When d_0/Λ increases, this mode shifts to the right and approaches the light line of n_0 whereas the second mode appears on the left when d_0/Λ=1.80.

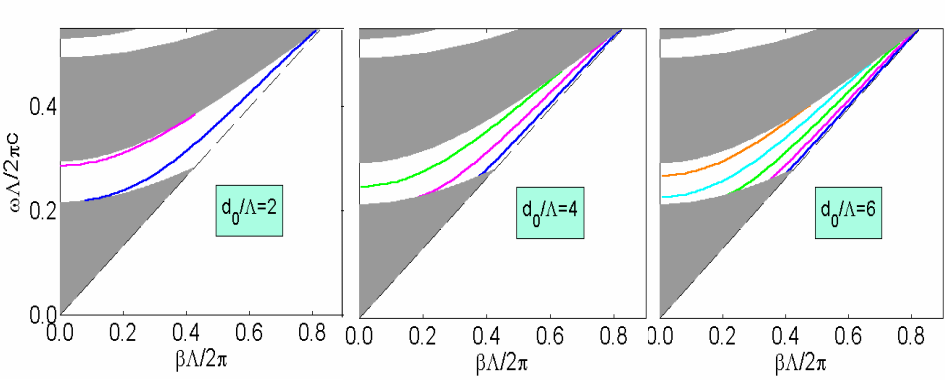

Fig. 4.24. Dispersion relation for the guided modes of the proposed waveguide (n_0=n_L=1.5, n_H=2.5, and d_H/Λ=0.45) for different core thickness d_0/Λ. Each line corresponds to one mode. The projected band structure of the OM is also depicted.

When the core thickness increases further, all the modes shift towards the light line and draw closer together as new modes appear on the left. This effect is better illustrated in Fig. 4.25a where β is represented for different d_0/Λ, for a constant normalized frequency $\omega(\Lambda/2\pi c)$=0.29. When d_0/Λ increases, β increases and asymptotically approaches a limit value corresponding to the light line for this frequency, which is $\beta(\Lambda/2\pi)$= 0.435.

The confinement gives important information about the modes as it indicates the fraction of the energy that is confined within the core layer. Fig. 4.25b shows the confinement of the modes represented in Fig. 4.25a. When d_0/Λ increases, the confinement of the modes increases and gets closer to

UNIVERSITAT ROVIRA I VIRGILI
DESIGN, FABRICATION AND CHARACTERIZATION OF POROUS SILICON MULTILAYER OPTICAL DEVICES
Elisabet Xifré Pérez
ISBN: 978-84-691-0362-3/DL: T.2181-2007

100 %. This indicates that the modes that are closer to the light line have a higher confinement.

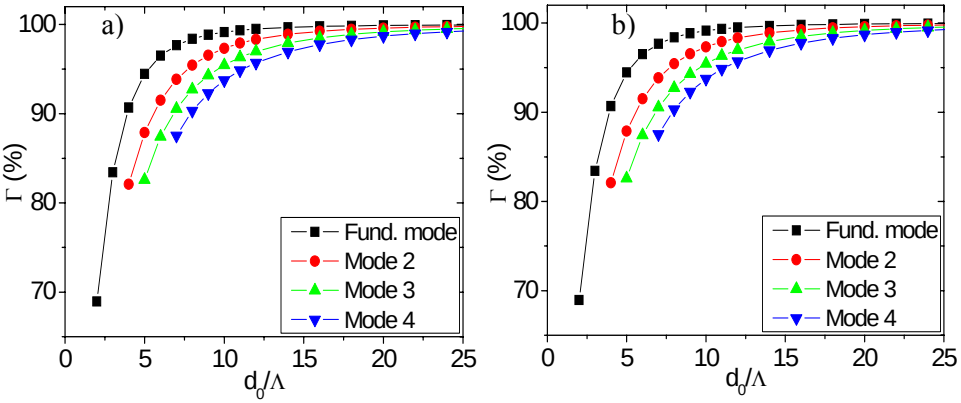

Fig. 4.25. Normalized surface-parallel wavevector $\beta(\Lambda/2\pi c)$ (a) and confinement Γ (b) for the first four guided modes as a function of the core thickness, for $\omega(\Lambda/2\pi c)$ =0.29. The dashed line in (a) indicates the value of $\beta\Lambda/2\pi c$ at the light line of n_0 for this frequency.

b) Analysis of the confinement for different DBR and OM cladding waveguides

In the framework of planar waveguides, a previous study [128] proposes a DBR cladding optimized for the propagation angle of the fundamental mode. However, the same study [128] also suggests that an OM might be more suitable for guiding more than one mode since it reflects the light regardless of the angle.The OM is indeed a particular case of DBR possessing an ORR. For this reason, in this section we analyze the performance of two different DBRs as cladding for waveguides and compare it with the performance of the OM waveguide. The three structures compared in this section (OM and DBRs) fulfill the condition that they have the same fabrication complexity: that is to say, they have the same refractive indices $n_0=n_L=1.5$ and $n_H=2.5$, the same number of periods (15) and the same period thickness (Λ).

UNIVERSITAT ROVIRA I VIRGILI
DESIGN, FABRICATION AND CHARACTERIZATION OF POROUS SILICON MULTILAYER OPTICAL DEVICES
Elisabet Xifré Pérez
ISBN: 978-84-691-0362-3/DL: T.2181-2007

The criterion to choose the first DBR cladding (DBR_1) is based on the fact that to have good light guiding and confining properties it is desirable that the region of forbidden frequencies would be as wide as possible. The DBR with the widest forbidden frequencies region is also the one with the widest frequency gap for normal incidence. This corresponds to the structure where the optical thicknesses of the two layers of the period are equal at normal incidence, that is $n_H d_H = n_L d_L$ and thus $d_H/\Lambda = 0.375$.

For the second DBR cladding (DBR_2) we have applied the criterion that the fundamental mode confinement at the studied core thickness range is maximum. For the studied frequency of $\omega(\Lambda/2\pi c)=0.29$, the center frequency of the OBG, this condition is given for $d_H/\Lambda = 0.60$.

The modal confinement of these three waveguide structures with different cladding is represented in Fig. 4.26. The first four guided modes for the central frequency of the OBG are analyzed in this figure. It can be observed that for all the modes, the OM and the DBR_2 cladding waveguides have a high confinement whereas the DBR_1 cladding waveguide has a lower confinement. Besides, for the DBR_1 cladding the modes only exist for a range of d_0/Λ. This happens because when d_0/Λ increases, β increases, making the mode lie within the allowed region (the gray region in the PBS). This means that the light is no longer confined by the cladding. This is a consequence that there are propagating angles for that frequency not supported by the DBR waveguide.

Fig. 4.26 also shows that, in general, the confinement of the OM is very similar to the confinement of DBR_2. For the four modes and most of the core thicknesses the confinement of DBR_2 is slightly higher except for some particular cases. The confinement of the OM is higher than the one of DBR_2 in the case of small core thickness. The higher the mode order, the wider the range of d_0/Λ where the confinement of the OM is higher. The confinement of DBR_1 is lower in all cases than the confinement of the OM and in some particular cases it is higher than the confinement of the DBR_2.

UNIVERSITAT ROVIRA I VIRGILI
DESIGN, FABRICATION AND CHARACTERIZATION OF POROUS SILICON MULTILAYER OPTICAL DEVICES
Elisabet Xifré Pérez
ISBN: 978-84-691-0362-3/DL: T.2181-2007

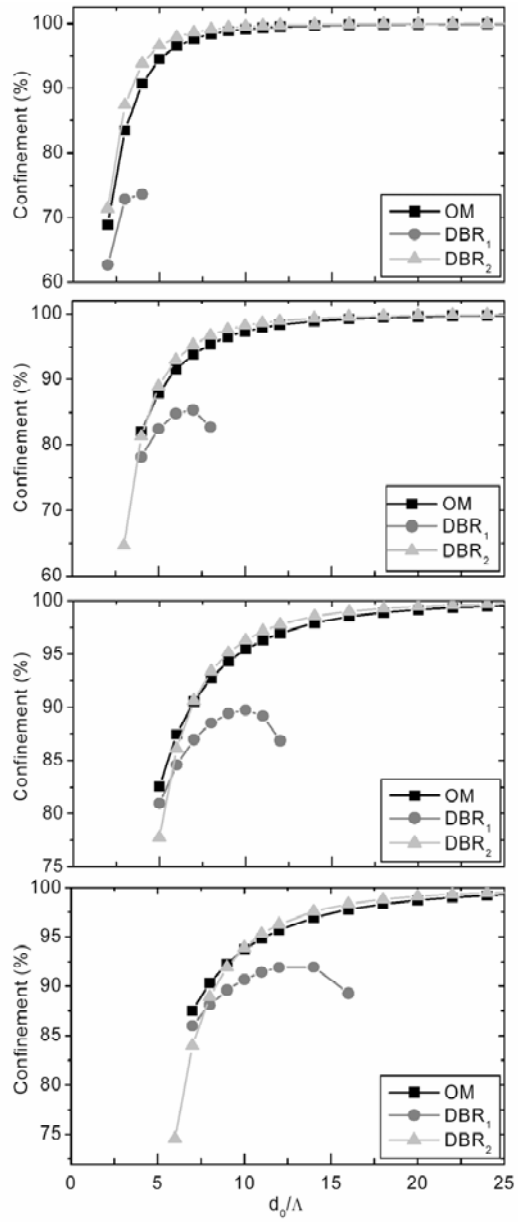

Fig. 4.26. Confinement of the four first modes of the OM cladding waveguide and the two DBR cladding waveguides as a function of the core thickness for $d_0/\Lambda=15$ and $\omega(\Lambda/2\pi c)=0.29$.

UNIVERSITAT ROVIRA I VIRGILI
DESIGN, FABRICATION AND CHARACTERIZATION OF POROUS SILICON MULTILAYER OPTICAL DEVICES
Elisabet Xifré Pérez
ISBN: 978-84-691-0362-3/DL: T.2181-2007

4.2.2.4. Modes of the multilayer waveguide

The modes of the multilayer waveguides have been studied using the PBS of the multilayer cladding. In this section, the modes that exist for the multilayer structure waveguide are discussed depending on their position in the PBS of the multilayer.

For this discussion, we study the modes of the waveguide whose refractive indices for the OM are the ones used in the previous section: n_H=2.5 and n_L=1.5 [174]. We concretely study the different types of modes that can exist in this waveguide for the central normalized frequency within the OBG: $\omega(\Lambda/2\pi c)$=0.29. The modal analysis of the waveguide structure has been carried out with the transfer matrix method applied to planar multilayer optical waveguides [175]. The values of β that satisfy the modal condition [eq. 26 in 175] have been calculated. For this discussion the core thickness d_H/Λ=5 has been chosen. Although this study has been done for d_o/Λ=5, the behavior of the modes is the same for any core thickness.

At this frequency and for this core thickness there are seven different β that satisfy the modal condition. The position of these modes within the PBS is given in Fig. 4.27.

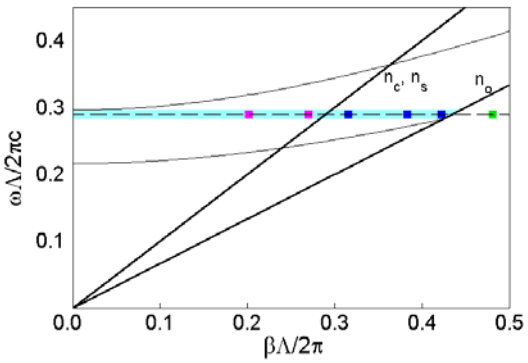

Fig. 4.27. PBS of the studied multilayer with the modes for d_0/Λ=5. The OBG is represented by a light gray area. The points indicate all the possible modes for ω=0.29·($\Lambda/2\pi c$). The diagonal lines are the light lines of the core and the bounding media.

UNIVERSITAT ROVIRA I VIRGILI
DESIGN, FABRICATION AND CHARACTERIZATION OF POROUS SILICON MULTILAYER OPTICAL DEVICES
Elisabet Xifré Pérez
ISBN: 978-84-691-0362-3/DL: T.2181-2007

The two modes with the lowest β are the ones with $\beta(\Lambda/2\pi)=0.2011$ and 0.2698. They lie above the light line for n=1 (corresponding to either bounding medium n_s, n_c[175]) but inside the OBG These are radiation modes since, although they are confined within the core because of the photonic crystal effect of the OM, they can propagate in the cover or substrate, as it can be seen in Fig. 4.28.

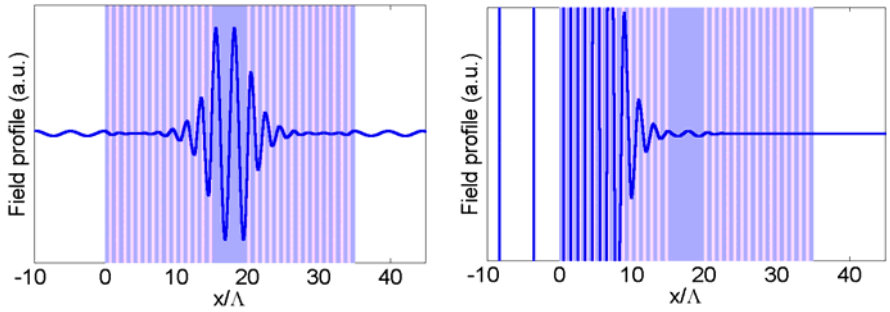

Fig. 4.28. Field profile of the two modes with $\beta(\Lambda/2\pi)=0.2011$ and 0.2698. Their corresponding β are lower than n_s,n_c. As can be observed, their are radiant modes.

The next three modes with $\beta(\Lambda/2\pi)=0.3153$, 0.3832, and 0.4219 lie below the light line of the bounding media and above that of the core. Fig. 4.29 shows that the field is confined within the core and is evanescent in the bounding media. Furthermore, a fundamental model and successive harmonics can be recognized.

UNIVERSITAT ROVIRA I VIRGILI
DESIGN, FABRICATION AND CHARACTERIZATION OF POROUS SILICON MULTILAYER OPTICAL DEVICES
Elisabet Xifré Pérez
ISBN: 978-84-691-0362-3/DL: T.2181-2007

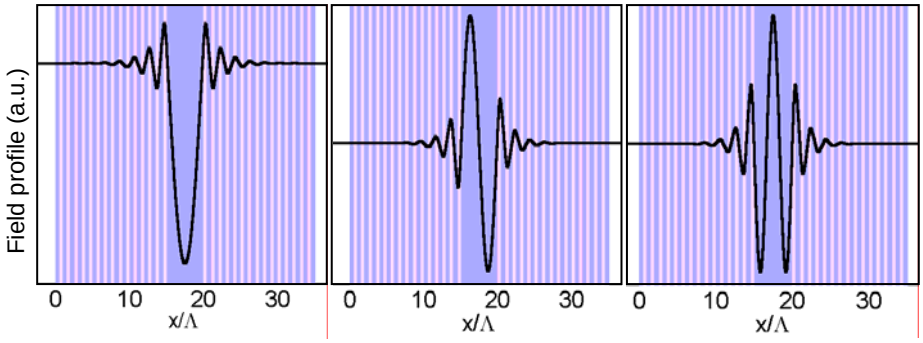

Fig. 4.29. Field profile of the three modes with $\beta(\Lambda/2\pi)$=0.3153, 0.3832, and 0.4219. Their corresponding β are between the light lines of the core and of the cover/substrate (n_s,n_c<β<n_o). They are guided modes.

Finally, the modes below the light line of the core, that is $\beta(\Lambda/2\pi)$=0.48081 and 0.48082, show an evanescent field in the bounding medium and in the low-index material (see Fig. 4.30). Even though these modes are confined in the multilayer structure cannot be considered as guided modes by the effect of the OM.

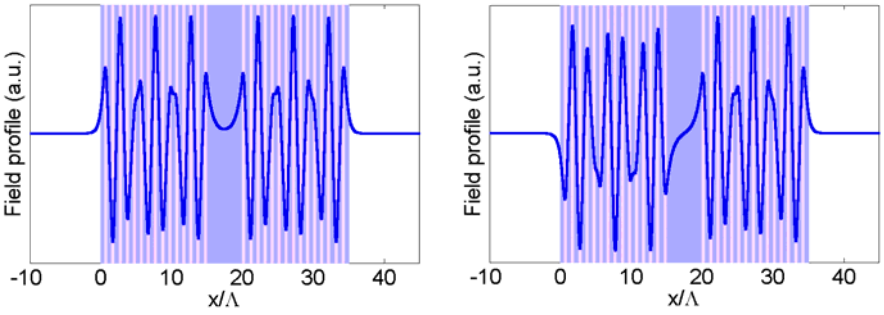

Fig. 4.30. Field profile of the two modes with $\beta(\Lambda/2\pi)$=0.48081, 0.48082. Their corresponding β are higher than n_o. As can be observed, they are not guided modes.

UNIVERSITAT ROVIRA I VIRGILI
DESIGN, FABRICATION AND CHARACTERIZATION OF POROUS SILICON MULTILAYER OPTICAL DEVICES
Elisabet Xifré Pérez
ISBN: 978-84-691-0362-3/DL: T.2181-2007

4.3. Conclusions

The simulation of different optical devices based on multilayers has been realized using the different programs presented in the previous chapter. These optical devices are omnidirectional mirrors and waveguides. All of them have been designed for 1.55 μm applications and the use of porous silicon for their fabrication has been discussed.

Omnidirectional mirrors are the optical devices most widely studied in this work. The periodic structure is the most commonly used for the formation of omnidirectional mirrors and the different parameters that influence on its omnidirectional bandgap have been studied. But the limited range of refractive indices obtainable with porous silicon restricts the omnidirectional bandgap width of this structure. One of the objectives of this work was to obtain porous silicon omnidirectional mirrors with a wide bandgap, as is required by different omnidirectional mirrors applications. For this reason different multilayer structures have been studied and proposed. The chirped structure, reported by a few groups, can be a suitable structure with a wider omnidirectional bandgap, just as has been demonstrated in this study. Besides, three different omnidirectional mirror structures have been proposed. It has been demonstrated that all of them have an omnidirectional bandgap wider than the one of the chirped structure.

The first structure proposed is the random structure where the thickness of the high refractive index layer varies randomly in the multilayer structure. The different parameters that influence on the omnidirectional bandgap width have been discussed and it has been demonstrated to have a wider omnidirectional bandgap than the periodic and the chirped structures. The main disadvantage of this structure is that the results strongly depend on many different parameters, which hinders its design. The study of this structure has lead us to propose two other mirror structures that have an enlarged omnidirectional bandgap and have very simple design rules: the balanced and the unbalanced structures. Both mirror structures consist of a few periodic multilayers (substuctures) stacked together where the period is different for each one, being their bangaps centered at different wavelengths. The bandgap of the

UNIVERSITAT ROVIRA I VIRGILI
DESIGN, FABRICATION AND CHARACTERIZATION OF POROUS SILICON MULTILAYER OPTICAL DEVICES
Elisabet Xifré Pérez
ISBN: 978-84-691-0362-3/DL: T.2181-2007

mirror structure is the union of the bandgaps of the substructures that make it up. The number of substructures stacked together is not limited, so wide omnidirectional bandgaps can be obtained without the limitation of the refractive index range. Whereas the substructures of the balanced mirror have the same number of periods, in the unbalanced mirror the first and the last substructures have more periods than the others. It has been demonstrated that the omnidirectional bandgap of both structures is wider than the ones obtained with the periodic and the chirped structures.

Porous silicon waveguides have been also theoretically studied. First, waveguides based on total refractive index have been analyzed for 1.55 μm applications, and the influence of the refractive indices and the core thickness on the number of modes has been studied. It has been theoretically demonstrated that a porous silicon multilayer may be used as a waveguide for 1.55 μm applications. The analysis of waveguides with different core thickness has demonstrated that when the thickness increases, the number of TE modes increases. Four waveguides with the same refractive indices but with different core thickness have been proposed. The dispersion relations of these waveguides have been presented and the cutoff wavelength of the modes allowed in the waveguide has also been studied for different refractive indices of core and cladding. It has been demonstrated that, for a fixed core thickness, different refractive indices resulting in the same numerical aperture have the same cutoff wavelengths.

However, the most widely analyzed waveguide structure has been the one where the confinement of the light is based on the properties of photonic crystals, as a multilayer is in fact a one-dimensional photonic crystal. In these waveguides, the multilayer is the cladding. In concrete, we have studied the use of omnidirectional mirrors and DBR to be used for the cladding. Three different types of modes have been observed depending on their position in the PBS of the multilayer cladding. It has been demonstrated that the guided modes are the ones with $n_s,n_c<\beta<n_o$. The influence of different parameters of the waveguide structure on the modes and the modal confinement has been studied. We have observed that the core refractive index that leads to the highest confinement is

UNIVERSITAT ROVIRA I VIRGILI
DESIGN, FABRICATION AND CHARACTERIZATION OF POROUS SILICON MULTILAYER OPTICAL DEVICES
Elisabet Xifré Pérez
ISBN: 978-84-691-0362-3/DL: T.2181-2007

$n \leq 1.5$. It has been observed that when the core thickness increases, the β of the modes gets closer to the light line and the confinement increases getting closer to 100 %. This indicates that the modes that are closer to the light line have a higher confinement. Besides, the increment of core thickness results in the increment of the number of modes, the same that happened with TIR waveguides. Finally, the confinement of the OM cladding waveguide was analyzed with respect to two other different DBR cladding waveguides with the same fabrication complexity. DBR_1 was chosen to present the widest forbidden frequencies region. The second DBR (DBR_2) is the one with the maximum fundamental mode confinement for the studied frequency. Analyzing the confinement for the four first modes of these three structures, we have concluded that in general, for all the modes, the OM and the DBR_2 cladding waveguides have a higher confinement than the DBR_1 cladding waveguide. Besides, for the DBR_1 cladding the modes only exist for a range of d_0/Λ. The confinement of the OM is very similar to the confinement of DBR_2, being for the DBR_2 slightly higher except for some particular cases. The confinement of the OM is higher for the smallest core thicknesses.

From these results, it can be said that the OM cladding might be a good trade off between the different types of DBR. The OM cladding offers the possibility of having a high confinement for a certain number of modes even with a small core thickness, what permits a simpler fabrication complexity, as the overall thickness of the waveguide can be smaller.